TRANSPARENT
PROCESS

THE
EMBO
JOURNAL

The nascent polypeptide-associated complex is a key regulator of proteostasis

Janine Kirstein-Miles[1,4], Annika Scior[2,3,4], Elke Deuerling[2,*] and Richard I Morimoto[1,*]

[1]Department of Molecular Biosciences, Rice Institute for Biomedical Research, Northwestern University, Evanston, IL, USA, [2]Department Molecular Microbiology, University of Konstanz, Konstanz, Germany and [3]Department of Molecular Microbiology, Konstanz Research School Chemical Biology, Konstanz, Germany

The adaptation of protein synthesis to environmental and physiological challenges is essential for cell viability. Here, we show that translation is tightly linked to the protein-folding environment of the cell through the functional properties of the ribosome bound chaperone NAC (nascent polypeptide-associated complex). Under non-stress conditions, NAC associates with ribosomes to promote translation and protein folding. When proteostasis is imbalanced, NAC relocalizes from a ribosome-associated state to protein aggregates in its role as a chaperone. This results in a functional depletion of NAC from the ribosome that diminishes translational capacity and the flux of nascent proteins. Depletion of NAC from polysomes and re-localisation to protein aggregates is observed during ageing, in response to heat shock and upon expression of the highly aggregation-prone polyglutamine-expansion proteins and Aβ-peptide. These results demonstrate that NAC has a central role as a proteostasis sensor to provide the cell with a regulatory feedback mechanism in which translational activity is also controlled by the folding state of the cellular proteome and the cellular response to stress.

Introduction

To establish and maintain a functional proteome, several cellular processes have to be spatially and timely coordinated. These include the synthesis of new proteins to control the influx into the proteome as well as protein folding, modification, transport and turnover to regulate the localisation, functionality and concentration of proteins. The pro-

*Corresponding authors. E Deuerling, Department Molecular Microbiology, Universitaetsstrasse 10, Box M 607, University of Konstanz, 78457 Konstanz, Germany. Tel.: +49 7531 882647; Fax: +49 7531 884036; E-mail: elke.deuerling@uni-konstanz.de or RI Morimoto, Department of Molecular Biosciences, Rice Institute for Biomedical Research, Northwestern University 2205 Tech Drive, Hogan 2-100, Evanston, IL 60208, USA. Tel.: +1 847 491 3340; Fax: +1 847 491 4461; E-mail: r-morimoto@northwestern.edu
[4]These authors contributed equally to this work

cesses work in concert and form an interconnected network termed proteostasis. There is a constant need to adapt proteostasis to changes in environmental conditions that may result in protein misfolding and aggregation. Such a regulatory circuit to adapt proteostasis to protein-folding stress in the endoplasmic reticulum (ER) is the unfolded protein response (UPR). Besides the induction of ER-specific chaperones, the UPR also leads to the attenuation of global protein synthesis via phosphorylation of eIF2α (Walter and Ron, 2011). A reduction of protein synthesis aids in restoring proteostasis by reducing the chaperone load.

A similar phenomenon is described for heat shock that results in a transient attenuation of protein synthesis. The underlying mechanism has not been resolved yet. It has been speculated that a number of factors have a role in the translational regulation in response to heat shock including the initiation factors, eIF2α and eIF4F, the small ribosomal protein S6 and the chaperone Hsp70 (Panniers et al, 1994). Notably, Hsp70 interacts and cooperates with the two ribosome-associated chaperone complexes, the ribosome-associated complex (RAC; (Hundley et al, 2005; Otto et al, 2005; Jaiswal et al, 2011)) and the highly conserved nascent polypeptide-associated complex (NAC) to assist in the folding and maturation of newly synthesised proteins. Two recent findings indicate that ribosome-associated chaperones assist in the folding of ribosomal proteins and thus are important to maintain high translational activity (Albanese et al, 2010; Koplin et al, 2010). Since NAC binds to ribosomes and interacts with nascent polypeptides, a chaperone-like function of NAC was proposed (Bukau et al, 2000; Hartl and Hayer-Hartl, 2002; Wegrzyn and Deuerling, 2005).

NAC is comprised of an α-and β-subunit, of which the β-subunit is important for interaction with the ribosome (Reimann et al, 1999; Beatrix et al, 2000)(Supplementary Figure S6 and Figure 2F). The heterodimeric NAC complex exists in equimolar levels with the ribosome and associates with ribosomes in a 1:1 stoichiometry (Raue et al, 2007). NAC was originally described to interact with nascent polypeptides to prevent their inappropriate targeting to the endoplasmic reticulum (ER) in yeast (Wiedmann et al, 1994; Lauring et al, 1995; Powers and Walter, 1996; Moller et al, 1998; Raden and Gilmore, 1998; Wiedmann and Prehn, 1999), and depletion of the β-subunit induces the UPR in Caenorhabditis elegans embryos (Arsenovic et al, 2012). In addition, βNAC was identified as a target of caspase (Thiede et al, 2001) and NAC in nematodes was shown to have an apoptosis-suppressing activity (Bloss et al, 2003). Other suggested functions include a role for αNAC as a transcriptional regulator, whose activity may be affected by dimerisation with βNAC (Moreau et al, 1998; Yotov et al, 1998). Although, yeast deleted for one or all NAC-encoding genes are viable and exhibit no growth defects (Reimann et al, 1999; Koplin et al, 2010), the embryonic lethality of NAC mutants in C. elegans, Drosphila melanogaster and mice indicates an essential function of this complex in higher eukaryotes (Deng and Behringer, 1995; Markesich et al, 2000; Bloss et al, 2003).

It is not well understood, how cytosolic protein misfolding and aggregation upon acute and chronic stress affects *de novo* protein synthesis to rebalance proteostasis. The involvement of ribosome-associated chaperones in protein synthesis is intriguing as they could sense protein misfolding in direct proximity to the ribosome. Here, we show that the accumulation of misfolded and aggregated proteins with heat shock, ageing and other proteotoxic challenges result in sequestration of ribosome-associated NAC to the insoluble protein species. This recruitment leads to a depletion of NAC at the ribosome, where it is required to maintain high translation activity, and thus a decrease in the levels of translating ribosomes. Consequently, this titration of NAC contributes to a decline of protein synthesis with ageing and in response to proteotoxic challenges.

Results

NAC delays polyQ aggregation and is an important component of the cellular proteostasis network

NAC is an essential protein in the metazoans *C. elegans* and *D. melanogaster* (Markesich *et al*, 2000; Bloss *et al*, 2003). To circumvent the lethality of an NAC mutant, we examined whether RNAi-mediated knockdown of individual subunits or the entire complex would provide a conditional approach to elucidate NAC function in *C. elegans* (Kemphues *et al*, 1988). The efficiency of the RNAi-mediated knockdown of α + βNAC was demonstrated by western blot analysis after the animals were fed for 3 days with bacteria expressing α + βNAC dsRNA, leading to an 80% reduction in NAC

protein levels relative to control animals (Supplementary Figure S3B). We found that knockdown of βNAC by RNAi treatment causes a severe reduction of ∼90% of offspring. The reduction was less pronounced, but still significant by the knockdown of αNAC or both subunits (Supplementary Figure S2).

To examine whether NAC exhibits chaperone function in higher eukaryotes such as *C. elegans* that could contribute to the severe phenotype of the deletion mutation, we used an aggregation-prone polyQ-protein-folding sensor to assess the proteostatic environment upon depletion of NAC (Satyal *et al*, 2000; Morley *et al*, 2002). We employed a reporter construct containing 35 glutamine residues fused to YFP (Q35-YFP) to monitor the folding status *in vivo*. Q35-YFP expressed in the muscle cells of young adult animals (day 4) remains soluble and exhibits a diffuse fluorescence in all expressing cells ((Morley *et al*, 2002), Figure 1A). RNAi-mediated knockdown of αNAC and βNAC subunits individually and in combination caused both an early age of onset (day 4) and increased (sixfold) aggregation of Q35-YFP compared to the control (empty RNAi expression vector) (Figure 1A and B). The increased aggregation propensity of Q35-YFP upon knockdown of either αNAC, βNAC or in combination (α + βNAC) can be observed throughout the lifetime of the animal and attributed to the polyQ expansion alone as expression of YFP alone remains soluble under the same conditions (Supplementary Figure S1A–D and H). This increase in aggregation of Q35-YFP is similar to that observed upon knockdown of the cytosolic Hsp70 chaperones, *hsp-1*, *F11F1.1* and *F44E5.4* (Supplementary Figure S1E–G). These
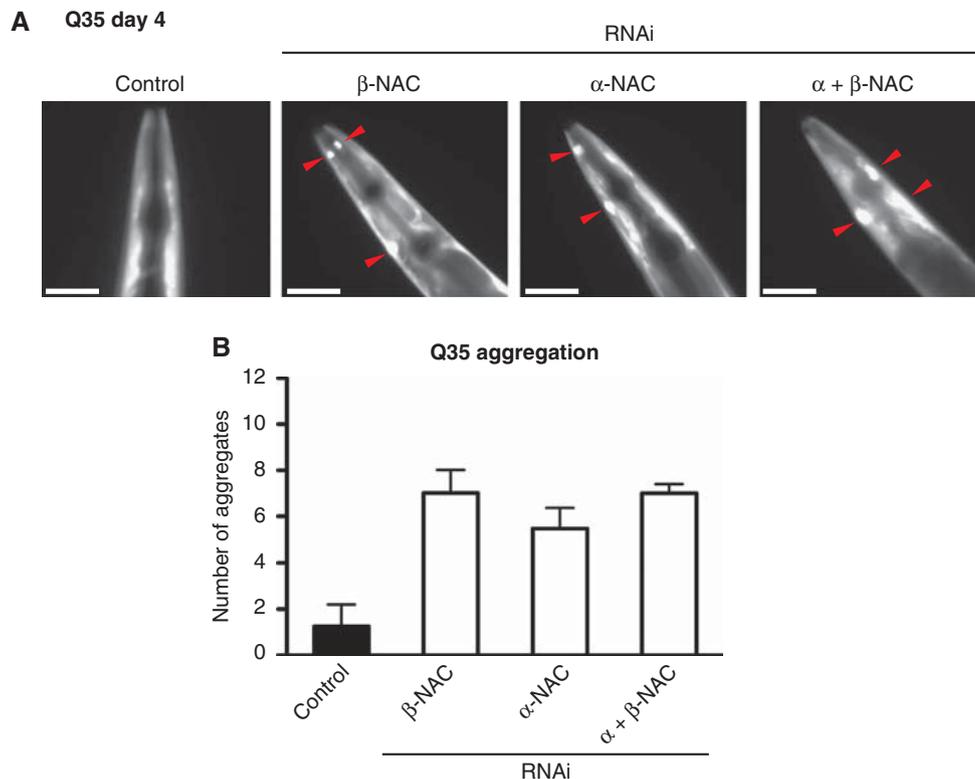

Figure 1 NAC prevents polyQ aggregation and is an important component of the cellular proteostasis network. (**A**) Depletion of NAC leads to a higher aggregation propensity of polyQ proteins. The aggregation propensity of the threshold polyQ model Q35-YFP expressed in muscle cells was analysed on day 4 upon knockdown of αNAC, βNAC and α + βNAC. The pictures show representative images of the head region. PolyQ aggregates are indicated by red triangles. The scale bars are 25 μm. (**B**) Quantification of the number of Q35 aggregates in the whole nematode. Error bars represent mean ± s.d. of 50 animals.

Table I Co-immunoprecipitation and LC-MS/MS analysis using NAC antibodies and a whole cell lysate of non-synchronized nematodes

Uniprot ID	Coverage	Peptides	MW	Score	Protein
Chaperones					
P09446	33.75	19	69.7	1798.77	HSP-1 (Hsp70)
O45246	6.07	3	70.4	280.75	C12C8.1 (Hsp70)
Q18688	25.07	17	80.2	1457.49	DAF-21 (Hsp90)
Q05036	1.16	1	86.8	70.23	C30C11.4 (Hsp110)
P54811	12.11	6	89.7	492.54	CDC-48.1 (p97)
P54812	9.88	5	89.6	463.49	CDC-48.2 (p97)
P34328	8.18	1	12.3	26.18	HSP-12.2 (sHsp)
Q20363	52.83	6	17.8	395.89	SIP-1 (sHsp)
O16259	14.06	3	36.9	266.24	STI-1 (STI-1)
P52015	47.37	8	18.4	1203.59	CYN-7 (cyclophilin; Peptidyl-prolyl *cis-trans* isomerase 7)
P52011	27.17	6	18.5	535.60	CYN-3 (cyclophilin; Peptidyl-prolyl *cis-trans* isomerase 3)
P52009	13.54	2	20.7	455.95	CYN-1 (cyclophilin; Peptidyl-prolyl *cis-trans* isomerase 1)
P52013	16.18	3	21.9	157.31	CYN-5 (cyclophilin; Peptidyl-prolyl *cis-trans* isomerase 5)
Q21993	6.58	1	17.1	43.66	PFD-5 (prefoldin)
NAC					
Q86S66	59.39	11	22.1	2081.83	Y65B4BR.5 (Nascent polypeptide associated complex subunit alpha)
Q18885	75.78	11	17.5	1547.63	ICD-1 (Nascent polypeptide associated complex subunit beta)
Ribosomal proteins					
P46769	38.77	9	30.7	782.57	RPS-0 (40S ribosomal protein SA)
P48154	31.91	9	28.9	525.56	RPS-1 (40S ribosomal protein S3a)
P51403	9.93	3	28.9	123.46	RPS-2 (40S ribosomal protein S2)
P48152	34.41	11	27.3	639.79	RPS-3 (40S ribosomal protein S3)
Q9N3X2	8.88	2	29.0	136.93	RPS-4 (40S ribosomal protein S4)
Q9NEN6	23.58	4	28.1	366.62	RPS-6 (40S ribosomal protein S6)
Q23312	28.87	6	22.0	269.19	RPS-7 (40S ribosomal protein S7)
P48156	34.62	5	23.7	622.88	RPS-8 (40S ribosomal protein S8)
P49196	7.86	2	15.1	123.04	RPS-12 (40S ribosomal protein S12)
P51404	31.13	4	17.3	473.23	RPS-13 (40S ribosomal protein S13)
P48150	47.37	6	16.2	502.79	RPS-14 (40S ribosomal protein S14)
Q9XVP0	23.84	3	17.2	378.45	RPS-15 (40S ribosomal protein S15)
Q22054	41.67	6	16.3	384.83	RPS-16 (40S ribosomal protein S16)
O01692	42.31	4	14.9	294.63	RPS-17 (40S ribosomal protein S17)
O18650	56.16	8	16.3	452.39	RPS-19 (40S ribosomal protein S19)
Q19877	23.78	3	15.9	211.43	RPS-23 (40S ribosomal protein S23)
O45499	20.51	2	13.2	109.40	RPS-26 (40S ribosomal protein S26)
Q93572	44.55	11	33.8	793.52	RPA-0 (60S acidic ribosomal protein P0)
O02056	22.03	7	38.6	307.06	RPL-4 (60S ribosomal protein L4)
P49405	53.24	12	33.4	1571.06	RPL-5 (60S ribosomal protein L5)
P47991	21.20	4	24.3	303.25	RPL-6 (60S ribosomal protein L6)
O01802	29.92	9	28.1	576.59	RPL-7 (60S ribosomal protein L7)
Q966C6	22.26	5	30.2	332.17	RPL-7A (60S ribosomal protein L7a)
Q95Y90	5.29	1	21.5	65.63	RPL-9 (60S ribosomal protein L9)
Q09533	5.14	1	24.7	58.27	RPL-10 (60S ribosomal protein L10)
P61866	25.45	4	17.8	317.40	RPL-12 (60S ribosomal protein L12)
P91128	3.86	1	23.7	35.55	RPL-13 (60S ribosomal protein L13)
Q9BL19	5.35	1	21.5	32.83	RPL-17 (60S ribosomal protein L17)
O45946	4.79	1	21.0	35.96	RPL-18 (60S ribosomal protein L18)
O44480	18.89	3	20.9	244.84	RPL-18A (60S ribosomal protein L18a)
P34334	25.47	3	18.3	115.65	RPL-21 (60S ribosomal protein L21)
P52819	16.92	2	14.9	250.21	RPL-22 (60S ribosomal protein L22)
P48162	16.33	2	16.7	187.10	RPL-25.1 (60S ribosomal protein L23a)
Q20647	23.29	3	16.3	182.85	RPL-25.2 (60S ribosomal protein L23a)
Q19869	7.75	1	16.1	65.83	RPL-26 (60S ribosomal protein L26)
P91914	36.03	5	15.7	458.20	RPL-27 (60S ribosomal protein L27)
Q21930	28.57	4	13.7	146.39	RPL-28 (60S ribosomal protein L28)
Q9U332	7.38	1	14.3	90.55	RPL-31 (60S ribosomal protein L31)
P34662	15.45	2	14.2	91.43	RPL-35 (60S ribosomal protein L35)
Translation factors					
Q9XWI6	2.07	1	83.1	101.49	EIF-3 (Eukaryotic translation initiation factor 3 subunit B)
P27639	4.48	2	45.4	50.21	INF-1 (Eukaryotic initiation factor 4A)
P34563	21.12	2	17.9	228.71	IFF-1 (Eukaryotic translation initiation factor 5A-1)
P53013	4.10	2	50.6	172.48	EFT-3 (Elongation factor 1-alpha)
P29691	10.09	8	94.7	609.84	EEF-2 (Elongation factor 2)
SRP					
P91240	1.73	1	71.4	52.44	F08D12.1 (Signal recognition particle 72 kDa protein homolog)

The table shows the identified protein interaction partners.

data are consistent with our proposal that NAC is a component of the cellular proteostasis network.

However, unlike the core chaperone machines that have ATP-dependent protein remodelling functions, NAC does not contain an ATPase domain, which suggests that NAC likely cooperates with other molecular chaperones to assist in maintaining proteostasis. To address this, we identified NAC-associated proteins by co-immunoprecipitation using NAC antibodies, from a whole-cell lysate of non-synchronized nematodes followed by LC-MS/MS analysis. In addition to the identification of a large number of ribosomal proteins and translation factors, that are known to either directly interact with NAC or are associated with the ribosome ((Koplin *et al*, 2010; del Alamo *et al*, 2011) Table I), we also identified specific members of the major chaperone families including Hsp70 (HSP-1 and C12C8.1), Hsp90 (DAF-21), Hsp110 (C30C11.4), sHsps (HSP-12.2 and SIP-1), p97 (CDC-48.1 and CDC-48.2), cyclophilins (peptidyl-prolyl cis-trans isomerase, CYN-1, CYN-3, CYN-5 and CYN-7) and prefoldin (PFD-5) (Table I). These data suggest that NAC could interact and cooperate with these chaperones to form functional networks to maintain proteostasis.

NAC associates with insoluble proteins during ageing

We next asked whether NAC interacts with endogenous protein aggregates, based on the polyQ data (Figure 1 and Supplementary Figure S1) and previous observations that human NAC associates with artificial insoluble β-sheet proteins (David *et al*, 2010; Olzscha *et al*, 2011). Ageing is associated with protein aggregation; therefore to directly test whether NAC also associates with the aggregated protein fraction, we prepared soluble, insoluble and total protein fractions from age-synchronized animals. The levels of α-and βNAC were determined by SDS–PAGE and subsequent western blot analysis using polyclonal antibodies against *C. elegans* α and βNAC. As a control for the fractionation and biochemical analysis, we collected samples of a *C. elegans* line expressing YFP, which is a stable protein and therefore expected to remain soluble throughout life. The overall levels of α and βNAC did not change during lifespan

(Figure 2A and Supplementary Figure S3), however, the relative amounts of α- and βNAC in the soluble fraction decreased substantially from day 3 to day 10 and shifted to the insoluble fraction, whereas the levels of YFP remained completely soluble during ageing (Figure 2A and B).

To visualise the subcellular localisation of NAC *in vivo* during ageing and to confirm our biochemical analysis, we performed immunostaining of *C. elegans* with the NAC antibodies. NAC is ubiquitous and distributed throughout the cytosol and nucleus of all somatic tissues and germ line cells (Supplementary Figure S4A). The nuclear localisation of NAC was confirmed by co-staining with DAPI and by subcellular fractionation into nuclei and cytosol by differential centrifugation, where NAC co-fractionated with the known nuclear and cytosolic proteins, Histone H3 and α-tubulin, respectively (Supplementary Figure S4 and B). It has previously been reported that βNAC localises to mitochondria in *C. elegans* embryos (Bloss *et al*, 2003), however we did not detect localisation of NAC to mitochondria using α + βNAC antibodies (Supplementary Figure S4C).

Next, we examined the *in vivo* pattern of NAC subcellular localisation during ageing in day 3, 7, 10 and day 16-old animals. We observed a dramatic shift on day 3 from a soluble distribution of NAC to the appearance of foci, likely corresponding to age-associated protein aggregation on day 7 (Figure 2C). These *in vivo* data confirm our biochemical observations that NAC shifts from the soluble to the insoluble aggregated protein fraction during ageing (Figure 2A and B).

### NAC is recruited to protein aggregates during ageing

We set out to test whether NAC co-aggregates with other proteins during ageing or is specifically recruited to aggregates directly or indirectly through interactions with other chaperones. To address this, we first established a protocol to isolate protein aggregates from aged nematodes and analysed the protein composition by mass spectrometry (LC-MS/MS). We identified 241 proteins (Supplementary Table S1) of which 178 had been previously identified as aggregation prone during ageing, confirming that our isolated protein fraction reflects a reliable spectrum of age-dependent

Figure 2 NAC shifts from a soluble ribosome-associated state to the insoluble fraction upon ageing. (**A**) The protein content of 100 mg (wet weight) synchronized days 3, 5, 7 and 10 old *C. elegans* cultures were fractionated according to their solubility (see Materials and Methods). The total, (not fractionated), soluble and insoluble fractions of all samples were subjected to SDS–PAGE and subsequent western blot analysis using antibodies against NAC and GFP/YFP. (**B**) The quantification of the relative signals for αNAC (left), βNAC (middle) and YFP (right) in each of the total (green), soluble (blue) and insoluble (red) fractions reveals that the total amount of NAC stays constant during ageing, whereas the amount in the soluble fraction decreases and concomitantly increases in the insoluble fraction. YFP serves as a control for a protein that remains soluble throughout the lifespan of the animal. (**C**) NAC localises to foci during ageing. Animals of days 3, 7, 10 and 16 were analysed using immunohistochemistry for NAC localisation. NAC localises to foci with the progression of ageing. The nucleus is highlighted with blue triangles and foci, probably representing protein aggregates, with white triangles. The scale bars are 10 μm. (**D**) Experimental set-up for the *in vitro* titration assay. (**E**) NAC is actively targeted to protein aggregates. The insoluble fraction from day 12-old animals was isolated, washed with detergents and subsequently incubated with the soluble fraction of day 3-old animals. Western blotting reveals that NAC is found in pre-wash insoluble fractions and that it can be removed from aggregates by washing with detergents and rebinds to post-wash aggregates after incubation with lysate. Aggregated proteins were then re-isolated from all three samples and analysed by SDS–PAGE with subsequent Coomassie staining and in parallel by western blot using NAC and RPL-17 antibodies. The signal intensities of sample 1 for both NAC and RPL-17 were each quantified and used to normalise the intensities for samples 2. (**F**) Cartoon of the ribosome associated chaperone complexes NAC and RAC. The α-subunit of NAC is depicted in green and the β-subunit in red. NAC binds to the ribosome in close proximity to the ribosomal exit site via its β-subunit, whereas both subunits contact the nascent polypeptide chain. We could identify DNJ-11 as the Hsp40 component of the RAC complex (shown in grey) by sequence alignments, the *C. elegans* Hsp70 partner is not known. (**G**) NAC is required for translation-competent ribosomes. Depicted are the polysome profiles starting with the 80 S peak (see Figure 3A for a complete representative polysome profile of *C. elegans*) of age-synchronized day 3-old *C. elegans* cultures upon RNAi of αNAC (green), βNAC (red) and the control (black). The quantification of the relative polysome fractions with respect to the total RNA of the αNAC (green) and βNAC (red) knockdowns compared to the control (black) is depicted on the right. Error bars represent mean ± s.d. of three independent experiments. (**H**) The knockdown of non-ribosomal chaperones does not lead to a decrease of polysome profiles. RNAi mediated knockdown of p97 (*cdc-48.1*; blue), Hsp110 (*C30C11.4*; grey) and sHsp (*hsp-12.6*; purple) does not affect the polysome profile compared to control animals (black) on day 3.

aggregation-prone proteins (Supplementary Table S1; proteins previously identified as aggregation prone are indicated (David *et al*, 2010)). Among the aggregated proteins are both subunits of the NAC complex, which is in agreement with our biochemical and cell biological observations that NAC exhibits an age-dependent shift from the soluble to the insoluble fraction (Figure 2A–C).

To analyse if NAC itself becomes insoluble during ageing or whether it is targeted to and co-localises with aggregates, we performed an *in vitro* titration experiment (Figure 2D and E).
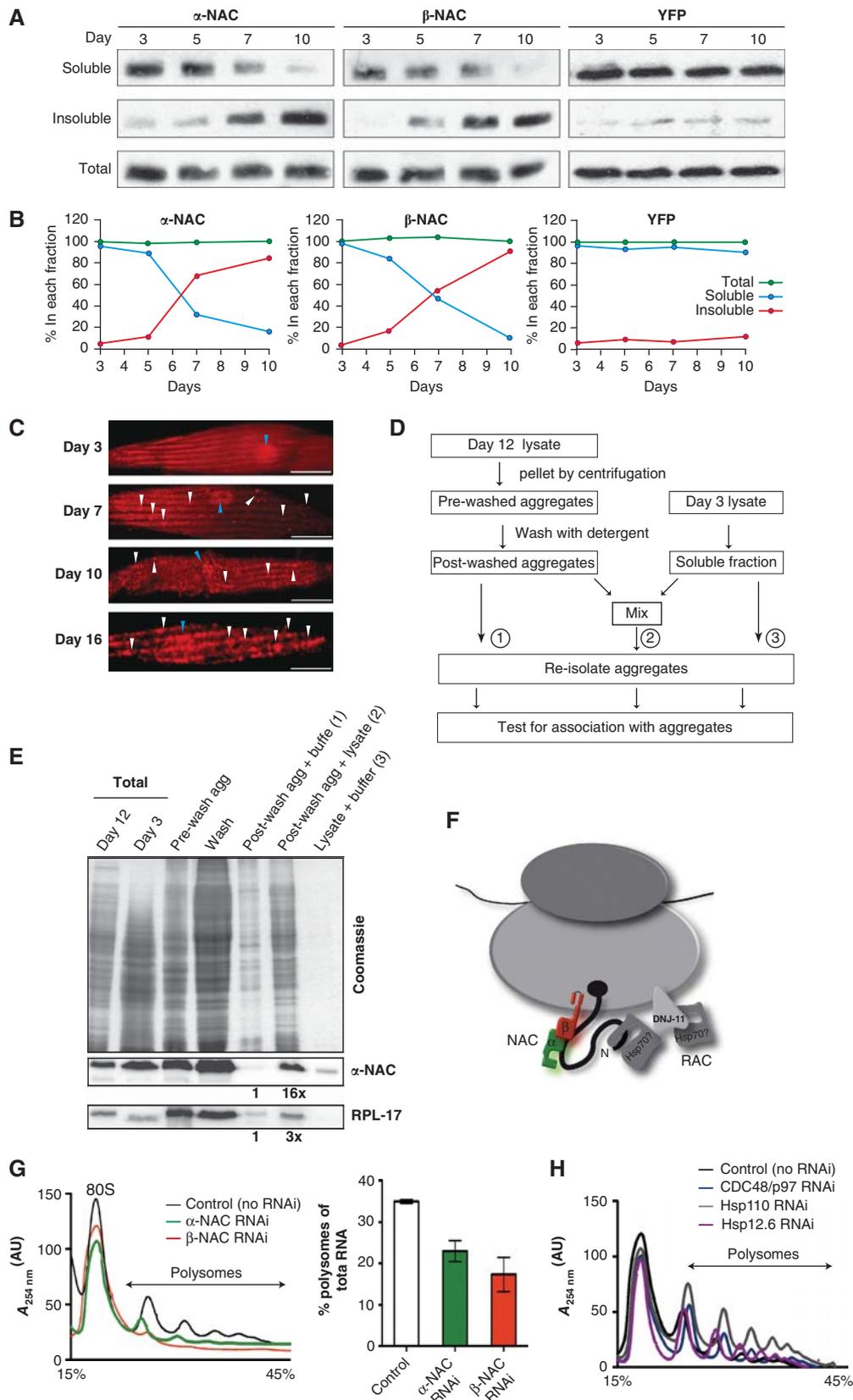
For this, we used the isolated insoluble protein fraction from day 12-old animals under low-salt and low-detergent conditions (pre-wash aggregates). The insoluble fraction was then subjected to detergent treatment to remove proteins that are loosely associated with aggregates for example, chaperones from those that are core constituents of the aggregate. The washed aggregates (post-wash aggregates) were then incubated with lysates from young day 3-old nematodes to allow rebinding and co-localisation of any proteins from the lysate with the aggregates isolated from aged animals (sample 2). For controls, we incubated post-wash aggregates or lysate with buffer (samples 1 and 3). All samples were then subjected to SDS–PAGE and the amount of NAC was analysed by immunodetection. We observed that NAC was present in the pre-wash aggregate fraction, in agreement with our previous observations (Figure 2A–C). However, after detergent treatment, NAC was efficiently removed from the pre-wash aggregates and found almost exclusively in the wash fraction, whereas only very little NAC remained in the post-wash aggregate fraction (Figure 2E). This suggests that NAC most likely binds weakly to the surface of aggregates. This finding is supported by the fact that soluble NAC can re-bind to post-wash aggregates from a lysate prepared from young nematodes. To test if NAC passively co-sediments with ribosomes into the aggregated fraction, we analysed the solubility of a ribosomal protein, RPL-17. While the amount of NAC increases about 16-fold, the level of the aggregation-prone RPL-17 (Supplementary Tables S1–3) increases only threefold (compare samples 2 versus 1 (Figure 2E)). A similar ratio (about threefold) was observed for another ribosomal protein, RPL-25 (data not shown). Thus, the interaction of NAC with insoluble proteins is not due to the aggregation propensity of ribosomes. Rather, we conclude that NAC is associated with aggregates and that it can cycle from a soluble ribosome-bound state of a lysate of young animals to ageing-induced protein aggregates.

Ribosome-associated chaperones modulate translation activity

The recent finding that ribosome-associated chaperones are involved in translational activity in *Saccharomyces cerevisiae* (Albanese *et al*, 2010; Koplin *et al*, 2010), prompted us to investigate the role of NAC in modulating translation activity in metazoans. We confirmed the interaction of NAC with ribosomes in *C. elegans* and found that *C. elegans* NAC associated with the ribosome in a salt-sensitive manner (Supplementary Figure S5B).

Next, we analysed whether NAC modulates translational activity in a metazoan as was observed in yeast (Koplin *et al*, 2010). A comprehensive and global approach to assess protein synthesis is achieved by the analysis of polysomes, which reflects the translation capacity of the cell. To examine the role of NAC in translation, we compared the polysome profiles of *C. elegans* depleted for α- or βNAC by RNAi knockdown experiments with those of *C. elegans* treated with the vector control (Figure 2F and G). *C. elegans* lysates from young (day 3) nematodes were fractionated using sucrose-density centrifugation and individual ribosome fractions were monitored by $A_{254\,nm}$ measurements. As equal absorption units were analysed on each gradient, the relative peak heights display the quantities of the individual ribosomal species. Compared to the control, the depletion of αNAC or βNAC

resulted in a substantial decline of polysomes up to 50% of the control (Figure 2G). To determine whether this decline in polysomes is specific to the ribosome-associated chaperone, we analysed whether the effects of knockdowns of other major chaperones were co-precipitated with NAC (Table I), but are not associated with the ribosome itself, including p97 (CDC-48.1 + CDC-48.2), Hsp110 (C30C11.4) and the small Hsp, HSP-12.6. Reducing the expression of these chaperones did not have significant effects on polysome formation in day 3-old nematodes (Figure 2H). Taken together, we conclude that the ribosome-associated chaperone NAC is an important modulator of translation activity in *C. elegans*.

Protein synthesis declines during ageing

Ageing is associated with an accumulation of misfolded proteins and a decline in the protein-folding capacity associated with a reduction in stress response pathways (Ben-Zvi *et al*, 2009; David *et al*, 2010). Our observation, that NAC is specifically and quantitatively sequestered by protein aggregates that accumulate during ageing (Figure 2A–C), led us to examine whether protein synthesis was also affected as a consequence. The translational capacity during ageing was analysed by comparing the polysome profiles in age-synchronized populations of *C. elegans* starting from day 2 of life through day 14 corresponding to the period of medium lifespan (Figure 3C and D and Supplementary Figure S7). Relative to an asynchronous population (Figure 3A and B) (comprising eggs, all larval stages (L1-L4) and adult animals), the amount of polysomes declined noticeably in synchronized animals beginning at an early age of day 2 (Figure 3C and D and Supplementary Figure S7). Quantification of the relative abundance of polysomes with respect to total RNA revealed that the polysome fraction declined by 87% during ageing between day 2 and day 10 (Figure 3D). This demonstrates a significant decrease in translational activity as *C. elegans* transitions from development into adulthood and senescence.

NAC is an important modulator of translation and protein aggregation upon heat shock

A similar response of a translational decline, albeit only transiently, occurs upon exposure to acute stress such as heat shock (Lindquist, 1980; Buchan and Parker, 2009). We asked whether NAC might also have a role in regulating translation upon heat shock. For that, we analysed the polysome profiles of young animals exposed to heat shock and observed a severe reduction in the polysome fraction (Figure 4A), consistent with previous observations in heat shocked *Drosophila* cells (Lindquist, 1980). We next analysed the recovery of polysomes following an acute stress upon depletion of the NAC complex. Upon heat shock of day 2 old animals for 1 h at 35°C and recovery for 24 h at 20°C, one set of animals was fed βNAC dsRNA expressing bacteria, whereas the control set was fed the empty RNAi vector-expressing bacteria. Whereas, the control animals recovered completely and exhibited a polysome profile typical of day 3-old nematodes (Figures 3D and 4A, Supplementary Figure S7), the animals depleted of βNAC during the recovery period showed a substantial reduction in polysome content (Figure 4A). These findings support our conclusion that NAC contributes to the active formation and maintenance of polysomes and translation.
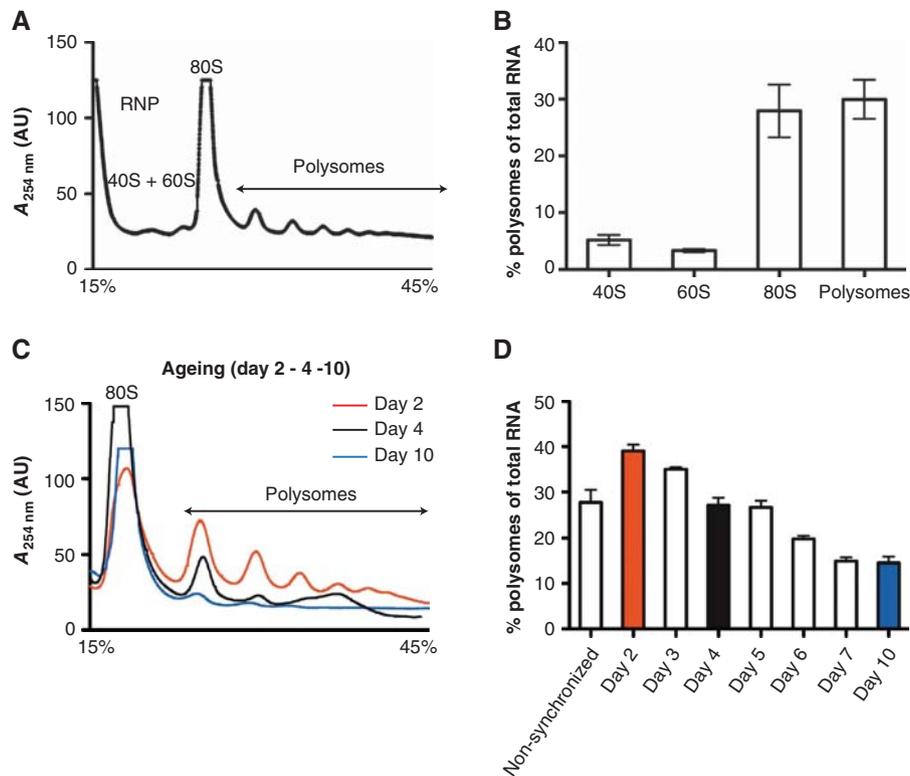
Figure 3 Protein synthesis declines during ageing. (**A**) Polysome profile of a non-synchronized *C. elegans* population. The relative abundance of 40 S, 60 S, 80 S ribosome species and the polysome fraction, respectively, is reflected in their absorption at 254 nm (y-axis). The x-axis depicts the sedimentation along a sucrose gradient from 15–45% (w/v). The depicted polysome profile is a representative of three independent analyses. (**B**) Quantification of the relative amount of 40 S, 60 S, 80 S and polysomes of a non-synchronized population (as shown in (a)) in % with respect to the total RNA. Three independent analyses were used to calculate and draw error bars representing mean ± s.d. (**C**) Polysome profiles of synchronized *C. elegans* populations of day 2 (red), day 4 (black) and day 10 (blue). The three profiles were aligned on the x-axis according to the sedimentation of their 80 S peak. The dashed line indicates the profile of the polysomes. (**D**) Quantification of the relative proportion of polysomes (in %) with respect to the total RNA level of non-synchronized and age-synchronized *C. elegans* cultures from day 2 to day 10. The polysome levels for days 2, 4 and 10 are highlighted in the same colour code as in (**C**). At least three independent analyses were used for each time point to calculate and draw error bars representing mean ± s.d.

We examined the effects of heat shock on the subcellular localisation of NAC. In animals exposed to heat shock (35°C for 30 min), we observed a dramatic change in the subcellular localisation of NAC (Figure 4B). NAC shifts from a soluble diffuse distribution to foci likely corresponding to heat shock-induced aggregates. This change in subcellular localisation is completely reversible in animals exposed to heat shock and allowed to recover for 24 h at 20°C (Figure 4B). To further demonstrate that the foci correspond to insoluble protein deposits, we performed immunofluorescence on nematodes expressing a luciferase-YFP (Luc-YFP)-folding sensor, which rapidly aggregates upon heat shock (Rampelt *et al*, 2012). Indeed, the NAC foci co-localise with the Luc-YFP foci upon heat shock (Figure 4B). In summary, these data show that NAC associates with protein aggregates *in vitro* and *in vivo*.

NAC is necessary for clearance of aggregates after heat shock

Based on our findings that NAC interacts with heat shock aggregates and is required to resume translation after heat shock (Figure 4A and B and Supplementary Table S2), we tested for a direct functional involvement of NAC to modulate heat shock aggregates. To address this, we investigated the ability of *C. elegans* to resolve protein aggregates after heat shock in the absence or presence of NAC. Day 2-old nema-

todes were exposed to heat shock for 1 h at 35°C and allowed to recover at 20°C for 24 h. Whereas control animals showed a 50% reduction of aggregates during recovery from heat shock, animals knocked down for βNAC during the recovery period showed only a moderate reduction of aggregates (Figure 4C). Importantly, NAC-depleted animals also failed to resume translation after heat shock (Figure 4A). To further analyse the contribution of NAC to the cellular folding conditions after heat shock, we employed the Luc-YFP-folding sensor (Rampelt *et al*, 2012), that is soluble in control conditions and aggregates rapidly upon heat shock (Figure 4B). Aggregation of Luc-YFP is reversible when animals are allowed to recover for 24 h at 20°C, but greatly impaired when depleted of βNAC during the recovery period (Figure 4D). Likewise, Luc enzymatic activity is only partially restored in animals fed *Escherichia coli* - expressing βNAC dsRNA during the recovery period (Figure 4D).

Taken together, these data reveal that recruitment of NAC to aggregates has two major consequences. First, there is less NAC available to function at the ribosome, which in turn contributes to decreased translational activity. Secondly, NAC is required for the prevention and/ or clearance of protein aggregates to rebalance proteostasis after stress. We propose that the functional recruitment of NAC to protein aggregates represents an active role in proteostasis to combat protein aggregation and to restore proteome balance.

NAC is required for survival of prolonged heat stress

The increased susceptibility for protein aggregation upon knockdown of the NAC complex poses the question how animals depleted for the NAC complex cope with prolonged heat stress conditions. We addressed this by exposing day 4- old nematodes, that were fed with *E. coli*-expressing αNAC, βNAC, α + βNAC and as controls *hsp-1* (Hsp70) and *age-1* dsRNA, to a severe heat stress of 6 h at 35°C followed by a recovery period of 24 h at 20°C. The control animals fed with *E. coli* expressing only the empty RNAi vector displayed a
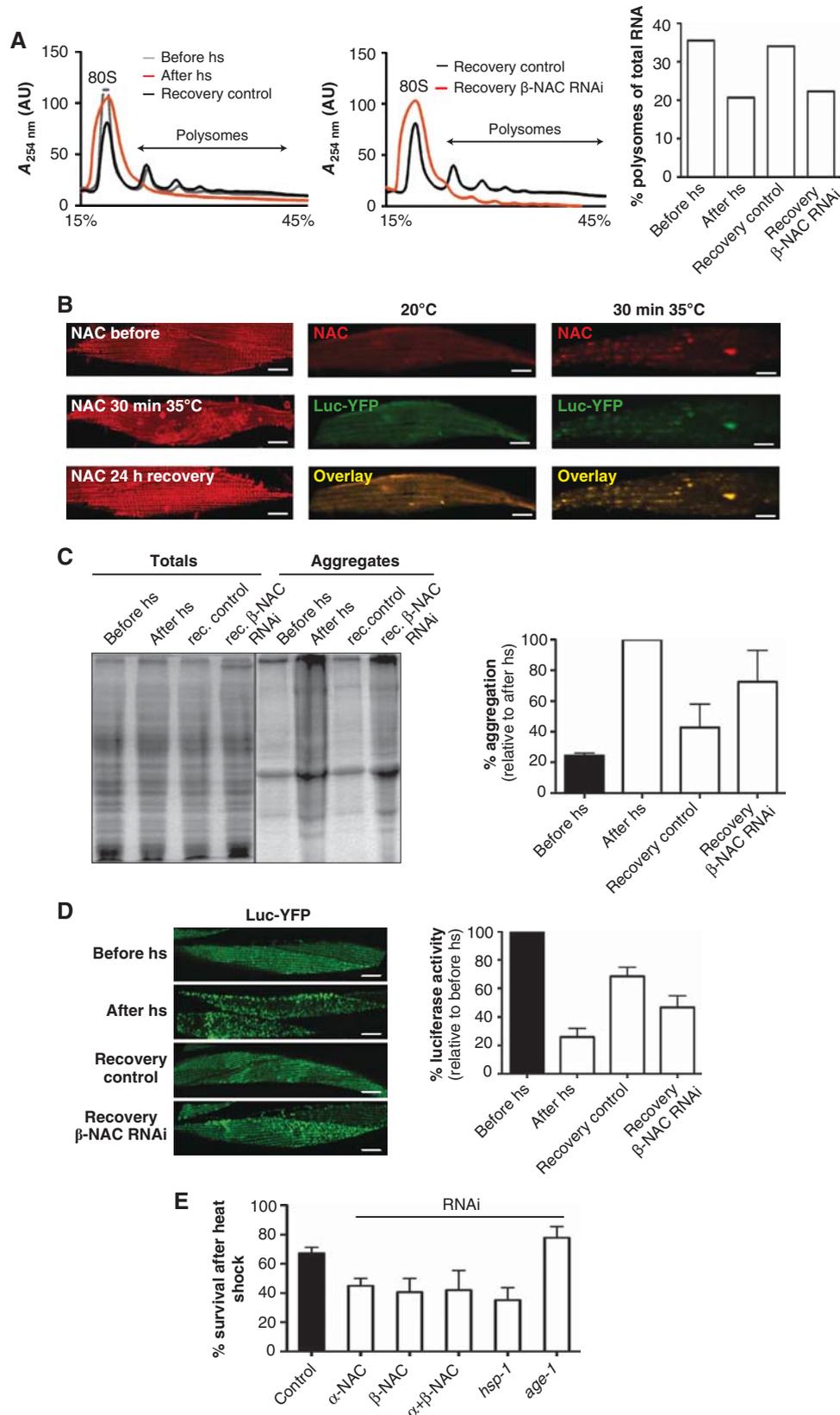
survival of ∼70%. As expected, animals depleted for the major Hsp70 chaperone *hsp-1* were severely affected and exhibited a lower survival of ∼30%. Likewise, knockdown of *age-1* that leads to increased lifespan and enhanced proteostasis (Dorman *et al*, 1995; Morley *et al*, 2002) showed increased survival rates of ∼80%. Knockdown of either or both NAC subunits had deleterious effects with survival rates of ∼40% (Figure 4E). These observations are in agreement with our findings of an absence of a compensatory effect by an upregulation of other cytosolic chaperones when NAC is depleted. For example, we did not observe an induction of either an inducible Hsp70 (*C12C8.1*) or small Hsp (*hsp-16.2*) reporter upon knockdown of NAC (Supplementary Figure S8).

In summary, the depletion of NAC has severe organismal defects upon proteotoxic challenges emphasising the important functions of this complex not only during embryogenesis (Bloss *et al*, 2003), but also during adulthood.

NAC is a sensor for proteotoxic stress

Our data point to an active targeting of NAC to protein aggregates. To gain further mechanistic insight on the order of events, we asked whether NAC dissociates from the ribosome at the same time when aggregates first appear and polysomes decline in response to a proteotoxic challenge. To address this, we employed heat shock as this proteotoxic condition allows for a precise monitoring of the kinetics of polysome formation and protein aggregation during the course of heat stress (Figure 5). An accumulation of protein aggregates can be observed within 10 min at 35°C that continues to increase at 30 and 60 min of heat shock (Figure 5B). The decline of polysomes, in contrast, is detected at 30 min of heat shock with a further decline at 60 min (Figure 5A). Thus, the formation of aggregates precedes polysome decline. These conditions allow for a kinetic assessment of NAC's relocalisation from a ribosome-bound soluble to an insoluble state, which then reduces translation.

To obtain further support, we performed immunofluorescence to investigate the relocalisation of NAC to protein aggregates as they appear and accumulate during the course of the heat shock. Antibodies against aggregation-prone ribosomal proteins RPL-4 and RPL-17 (see below,

Supplementary Tables S1–3) were used to distiguish whether NAC actively localises to heat shock aggregates or if NAC is passivly sequestered to protein aggregates as the ribosome itself undergoes aggregation. NAC foci formation can be observed within 10 min of heat shock and increases further at 30 and 60 min of heat shock (Figure 5C; foci are indicated with white arrow heads). By comparison, the ribosomal foci detected by immunostaining first appear at 60 min of heat shock (Figure 5C). We conclude from these results that NAC dissociates from the ribosome before the aggregation of the ribosome or its subunits. This is in agreement with our previous observation that ribosome-aggregation does not cause the co-sedimentation of NAC into the insoluble fraction (Figure 2E). Moreover, foci formation of NAC coincides with the observed appearance of protein aggregates, and the decline in polysomes begins after their dissociation from ribosomes to aggregates (Figure 5A and B). We conclude, therefore, that NAC could function as a sensor of proteotoxic stress in the cytosol and dissociate from the ribosome to aggregates to prevent the accumulation of additional aggregation-prone proteins.

NAC localisation to heat shock aggregates reduces the amount of NAC bound to the ribosome

We determined whether the localisation of NAC to heat shock aggregates results in a reduction of the ribosome-bound NAC using an *in vitro* titration experiment to demonstrate whether ribosome-bound NAC can specifically bind to aggregates and thus titrate NAC from ribosomes (Figure 5D; on the left). 80S monosomes and polysomes were isolated from day 3-old nematodes by a high-spin density gradient centrifugation and shown to have NAC bound to the ribosomes (Figure 5D; high spin sample 3). Next, we prepared a lysate from day 3-old animals that was depleted for ribosomes using a high-spin centrifugation step, and incubated at 42°C for 1 h to induce the formation of heat shock aggregates. These *in vitro* generated heat shock aggregates were shown to contain very low levels of NAC, as we used a ribosome-depleted extract of day 3-old nematodes (Figure 5D; low spin sample 1). To test whether NAC can be titrated from ribosomes to aggregates, we incubated isolated ribosomes bound to NAC with the *in vitro* formed heat shock aggregates that were NAC depleted (Figure 5D; sample 2). After incubation

Figure 4 NAC is important for the recovery from heat shock. (**A**) Heat shock of day 2 old *C. elegans* at 35°C for 1 h results in a reduction of polysomes (red). The condition before the heat shock (grey) and animals recovered for 24 h (black) serve as controls. The recovery from heat shock (1 h 35°C) is greatly diminished upon knockdown of βNAC (red) during the recovery period of 24 h compared to animals fed with RNAi bacteria expressing the empty vector (black; middle panel). A quantification of the polysome content with respect to the total RNA level is depicted on the right. (**B**) Heat shock causes reversible foci formation of NAC. Shown here is the localisation of NAC in a muscle cell of *C. elegans* grown at 20°C (top; left panel) and of *C. elegans* heat shocked for 30 min at 35°C (middle; left panel) and after 24 h recovery at 20°C (bottom; left panel). The NAC foci formed upon heat shock co-localise with aggregated luciferase-YFP. The images of the middle panel show the separate and overlay images of NAC (red) and Luc-YFP (green) at 20°C. The heat shock conditions are depicted on the right, respectively. The scale bars are 10 μm. (**C**) The gel shows the total (left lanes) and aggregated protein fractions (right lanes) of animals exposed to heat shock at 35°C for 1 h directly after heat shock and followed by a recovery at 20°C for 24 h upon knockdown of βNAC and of control animals, respectively. The quantification of the aggregated protein fraction of animals before heat shock (black), immediately after heat shock and animals that were fed bacteria-expressing βNAC dsRNA or the empty vector during the recovery period at 20°C for 24 h. The quantification of aggregation is normalised to the aggregation propensity after heat shock. Three independent experiments were used to calculate and draw error bars representing mean ± s.d. (**D**) Aggregation propensity of luciferase-YFP expressing animals before heat shock (top), immediately after heat shock (second from top) and after a recovery at 20°C for 24 h in control animals (third from top) or upon knockdown of βNAC during the recovery period (bottom). The scale bars are 10 μm. An analysis of enzymatic activity of luciferase of the luciferase-YFP expressing *C. elegans* before heat shock, immediately after heat shock and after a recovery period upon knockdown of βNAC or in animals fed the empty vector during the recovery period are shown on the right. The luciferase activity is normalised to the enzymatic activity before heat shock (black column). Three independent experiments were used to calculate and draw error bars representing mean ± s.d. (**E**) Knockdown of NAC reduces survival after heat shock. Animals grown on RNAi plates since L1 were subjected on day 4 to 6 h of heat-shock at 35°C followed by a recovery period at 20°C for 24 h. Survivors were scored after the 24 h recovery phase in three independent experiments with a total number of 120 animals for each condition. Error bars represent mean ± s.d. of the three independent experiments.

for 20 min, the protein aggregates were re-isolated by a low-spin centrifugation step and the ribosomes were subsequently isolated with a high-speed centrifugation step. The levels of NAC in the respective fractions were analysed by western blot analysis (Figure 5D). NAC was present in the aggregated protein fraction of the mixed sample (compare samples 2 and 3 after low spin; highlighted in red), due to its

dissociation from the ribosomes as we could detect a substantial loss of ribosome interaction in the presence of protein aggregates (Figure 5D; compare samples 2 and 3 after a high spin; highlighted in blue). In contrast, we did not observe aggregation of the ribosomal subunit, RPL-25, in this titration assay and the level of RPL-25 in the ribosomal fraction remained constant.
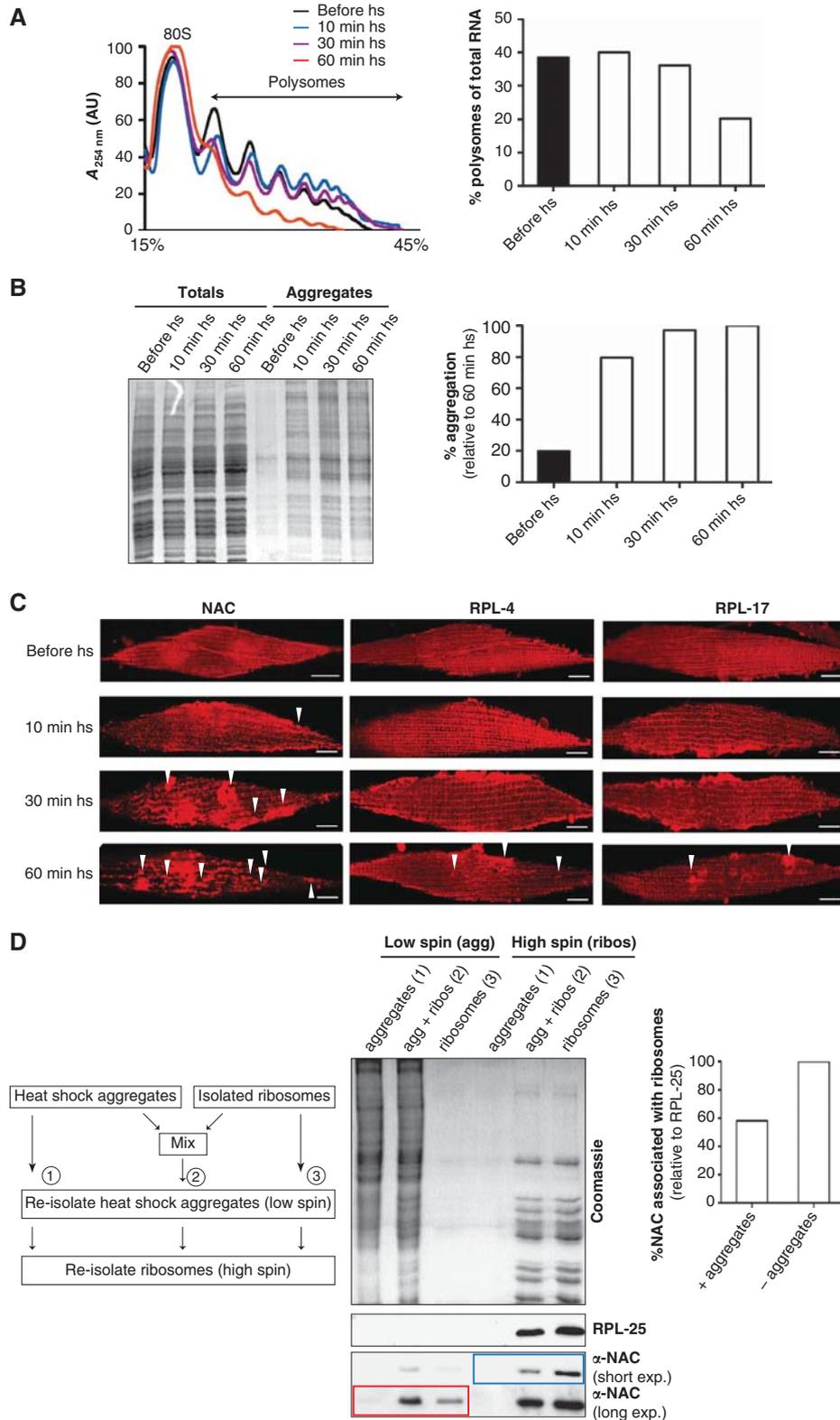
These *in vitro* titration experiments reveal that NAC partitions from a ribosome-associated state to insoluble protein aggregates, and that this shift results in the depletion of NAC from ribosomes. This shift in subcellular localisation of NAC could therefore represent an early response to an imbalance in protein-folding conditions in the cell.

Proteotoxic challenges reduce translational capacity

To test whether the re-localisation of NAC to protein aggregates extends to other conditions associated with proteotoxic stress and aggregation, we analysed the effects of ageing, heat shock and the expression of polyQ proteins (Supplementary Tables S1–3). In response to all forms of acute and chronic stress, we could identify NAC subunits among the aggregated proteins, which suggests that the shift from a soluble state to the insoluble protein fraction may represent a general response to imbalances of protein-folding conditions. We then analysed the composition of the aggregates formed during ageing with respect to the functional classes using the DAVID software (Huang *et al*, 2009a, b). Consistent with previous observations (David *et al*, 2010), proteins that are required for embryonic and larval development, the regulation of growth and translation are highly aggregation-prone during ageing (Supplementary Table S1 and Supplementary Figure S10). When comparing the functional annotation of the aggregation-prone proteins during ageing with aggregates formed upon heat shock and polyQ expression, we noticed that the same functional classes were over-represented (Supplementary Figure S10). Thus ageing, heat shock and polyQ expression lead to the misfolding and aggregation of a very similar subset of the proteome (Supplementary Tables S1–3 and Figure S10).

To address whether chronic proteotoxicity affects protein synthesis, we analysed the translational capacity of two well-established *C. elegans* models for proteotoxicity, expression of human Aβ-peptide and polyglutamine (polyQ) expansion proteins (Link, 1995; Morley *et al*, 2002). The expression of Aβ 1–42 leads to the accumulation of amyloidogenic deposits and age-dependent paralysis (Link, 1995; Cohen *et al*, 2006). Likewise, expression of polyQ exhibits both polyQ-length and age-dependent aggregation and toxicity (Morley *et al*, 2002). To test whether the chronic expression of Aβ and polyQ has global effects on protein synthesis, we analysed the polysome profiles in young animals to distinguish between proteotoxic and age-dependent effects. We observed a significant decline in the polysomes of synchronized populations of Aβ-peptide

and Q40-YFP-expressing *C. elegans* by day 3 and 4, respectively (Figure 6A and C). The decline was polyQ length-dependent, and observed only in animals expressing longer polyQ lengths on day 4 (Q40-YFP). The shorter polyQ variant (Q35-YFP) or YFP alone (Q0-YFP) did not exhibit protein aggregation (Figure 6B) or show any effects of translation at this specific time point (Figure 6A). This clearly demonstrates that the decline in protein synthesis is not caused by the expression of an artificial polyQ protein *per se*, but depends on the aggregation propensity of the polyQ protein. The expression of Aβ-peptide also resulted in a reduction in polysomes (Figure 6C). Thus, the decline of rotein synthesis is a common response to chronic proteotoxic challenges resulting in protein aggregation as observed before for acute stress (Figure 4).

To confirm whether this decline in translation activity is associated with the sequestration of NAC into protein aggregates, we examined the subcellular localisation of NAC by immunostaining in Aβ-peptide-expressing transgenic animals. Indeed, NAC also localised to foci, consistent with the expression of amyloidogenic protein aggregates (Figure 6D, right).

To examine the nature of NAC recruitment to Aβ-aggregates, we performed an *in vitro* experiment with recombinant functional NAC protein to test for interaction with cellular Aβ. Extracts from Aβ-expressing animals raised on *E. coli* expressing α- and βNAC ds RNA to reduce the levels of endogenous NAC were prepared. The NAC-depleted extract was used for a co-immunoprecipitation experiment with immobilised NAC antibodies, and subsequently pre-incubated with or without recombinant active NAC protein prior to addition of the Aβ-cell extracts. The immunoprecipitates were then subjected to SDS–PAGE and western blot analysis with the Aβ-specific antibody, 4G8. Recruitment of NAC to Aβ in the cell would predict co-precipitation of Aβ-protein in the NAC protein-containing sample. Indeed, Aβ was detected only in the NAC protein-containing sample (Figure 6E, right lane).

These results support our hypothesis that NAC interacts with Aβ in a functional state and is not sequestered into Aβ aggregates as a metastable, aggregation-prone protein. The Aβ peptide itself can be detected as multiple protein bands on SDS–PAGE, perhaps corresponding to multimers (Figure 6E, right lane). Due to the denaturing conditions of this SDS–PAGE analysis, it is not clear whether the recognised Aβ-species is an oligomer or higher-ordered aggregated

Figure 5 NAC acts as sensor for proteotoxic stress. (**A**) Analysis of polysome profiles of day 3-old nematodes before heat shock (black) after 10 (blue), 30 (magenta) and 60-min heat shock (red). The quantification of polysome profiles with respect to the total RNA is shown on the right. (**B**) The gel depicts the total protein levels (left lanes) and the aggregated proteins (right lanes) during the course of heat shock (hs). The time points are indicated on top. The quantification of the aggregated proteins of is shown on the right. The level of aggregation is normalised to the aggregation propensity at the 60-min time point of the heat shock. (**C**) Immunofluorescence of single muscles cells during the course of heat shock using antibodies against NAC (top row), RPL-4 (middle row) and RPL-17 (bottom row). The time points of heat shock (before, 10 min, 30 min and 60 min) are indicated on top. The foci probably representing insoluble protein are highlighted with white triangles. The scale bars are 10 μm. (**D**) Schematic presentation of the titration assay. Aggregates from heat-shocked animals were mixed with isolated ribosomes and incubated for 20 min. A parallel of the aggregates and isolated ribosomes were incubated with buffer and would serve as controls. All three samples were subjected first to a low spin to re-isolate protein aggregates and subsequently to a high spin to re-isolate ribosomes. The analysis of all fractions from the titration experiment by SDS–PAGE and subsequent Coomassie staining (top) and in parallel by western blot (bottom) using NAC and RPL-25 antibodies is shown in the middle panel. The αNAC signals are depicted in two different exposure times of the western blot (bottom 2 rows) for better visualisation of the signals. The low spin isolating the aggregated proteins is shown in the left lanes and the high spin isolating the ribosomes is shown in the right lanes. The individual fractions of the titration assay are depicted on top of the gel. A quantification of ribosome-associated NAC after the incubation with protein aggregates relative to the isolated ribosome sample is shown on the right. The quantification of αNAC is normalised to the protein levels of RPL-25 in both samples.
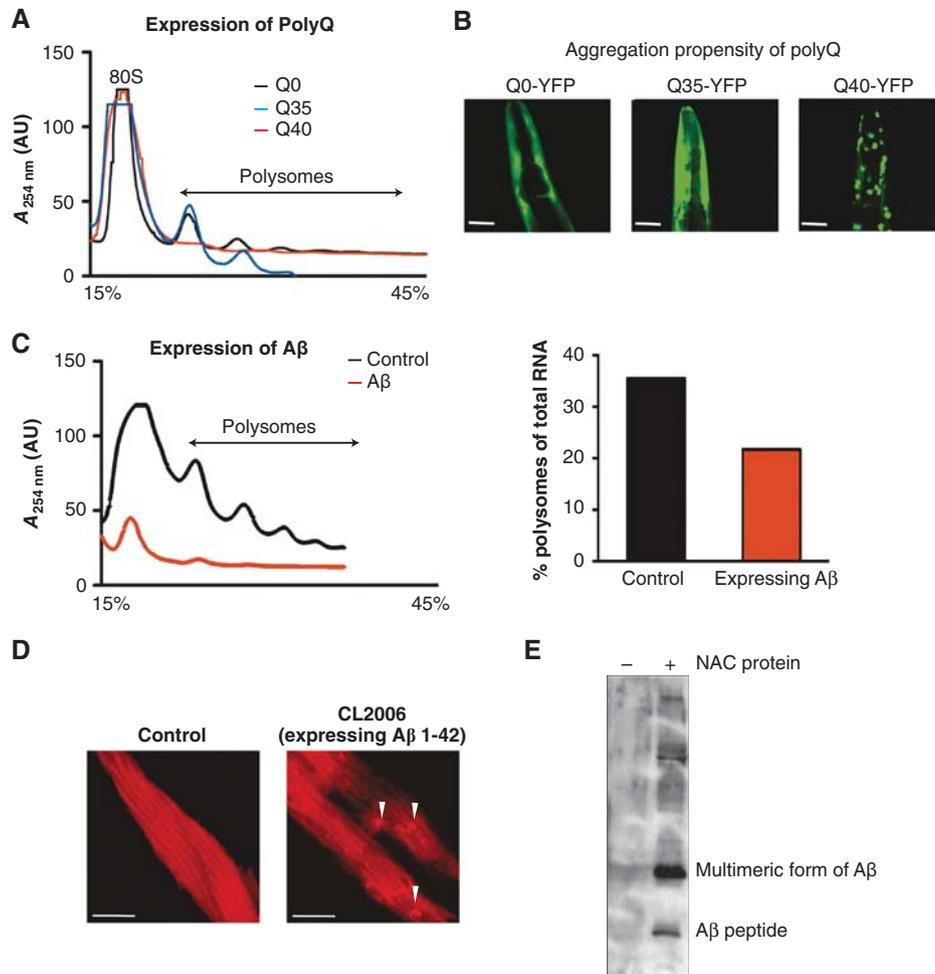
Figure 6 Polysome levels decline upon chronic stress. (**A**) Chronic stress: expression of 40 consecutive glutamines in the body wall muscle of *C. elegans* causes a reduction of polysomes. Depicted are the polysome profiles of day 4-old nematodes, which either express Q40-YFP (red), Q35-YFP (blue) or YFP alone (Q0-YFP, black) as control. (**B**) The images show the aggregation propensity of Q0-YFP (left), Q35-YFP (middle) and Q40-YFP (right) of the head region on day 4. Q40-YFP forms aggregates at day 4, whereas Q0-YFP and Q35-YFP remain soluble at that age (Morley *et al*, 2002) (see also Figure 1A and Supplementary Figure S1H). The scale bars are 25 μm. (**C**) Chronic stress: expression of Aβ causes a severe reduction of polysomes and 80 S levels. Depicted are the polysome profiles of Aβ-expressing nematodes (red) and the N2 wild type (control; black) on day 3. The quantification of the polysome content with respect to the total RNA level of is shown on the right. (**D**) Nematodes expressing the Aβ-peptide 1–42 in the body wall muscle cells were analysed by immunostaining with NAC antibodies. NAC forms foci in cells expressing Aβ most likely representing amyloid deposits (right). The control using wild type *C. elegans* (N2) is shown on the left. The scale bars are 10 μm. (**E**) Interaction of NAC and Aβ-peptide. Immobilised NAC antibodies were first incubated with recombinant NAC protein and the complex was subsequently incubated with extracts of an Aβ-expressing strain (CL2006) grown on α+βNAC RNAi. The precipitate was subjected to SDS–PAGE and western blot. The interaction was analysed using the Aβ-specific antibody 4G8. The antibody detected a strong signal for the Aβ-peptide and an additional signal of about 15 kDa probably representing oligomeric species of Aβ (right lane). A parallel, where no NAC protein was bound to the immobilised NAC antibodies, served as control and did not show an interaction with Aβ (left lane).

state. Likewise, we cannot rule out that NAC is recruited to Aβ-aggregates via interactions with other chaperones present in the cellular extract. Nevertheless, these data reveal that NAC is actively targeted to Aβ-aggregates due to its ribosome-independent function as a component of the proteostasis network.

Reduction of protein synthesis enhances proteostasis

Given that NAC is either associated with the ribosome, promoting protein synthesis and folding of the nascent chain, or alternatively associated with protein aggregates, we considered that this regulatory switch might serve to adjust protein synthesis and thus maintain proteostasis. Depletion of NAC from its ribosomal function by

sequestration to aggregates causes a decline in polysome formation (Figures 5 and 6) and hence, the attenuation of protein synthesis. One consequence of this would be a reduced flux of *de novo* synthesised proteins. This would allow the quality control system to re-establish the proteostatic balance of cells that encounter proteotoxic challenges. To address this, we attenuated protein synthesis by RNAi-mediated knockdown of the translation initiation factors, eIF4G (*ifg-1*) and eIF4E (*ife-2*) in the Q35-YFP protein aggregation model. These RNAi experiments were performed with L4 stage animals, because these factors are essential for development. We observed a substantial reduction in Q35-YFP aggregation of the pre-existing Q35-YFP protein level (Figure 7A and B). This effect was not due to differences in
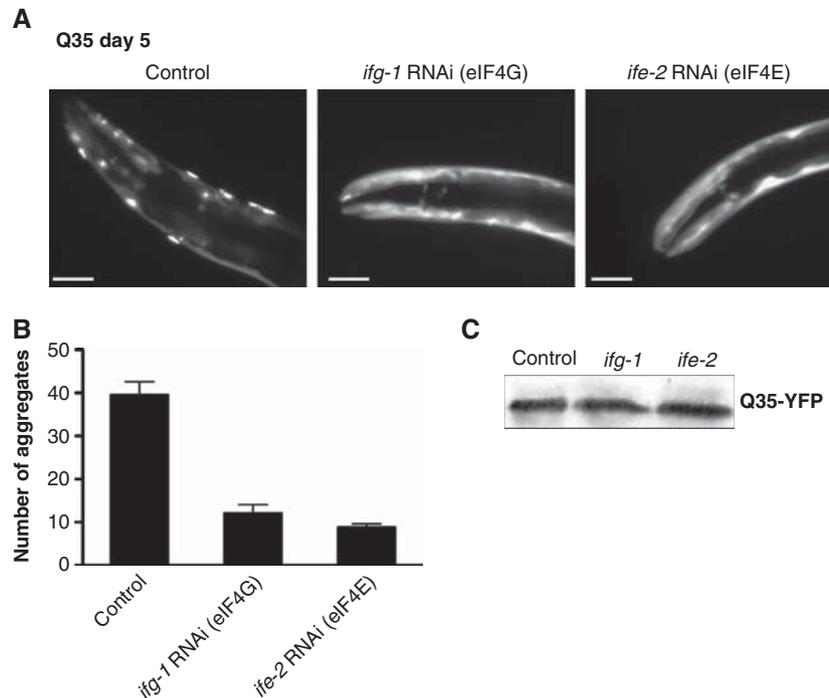
Figure 7 Reduction of translation initiation enhances proteostasis. (**A**) The knockdown of translation initiation factors eIF4G (*ifg-1*) and eIF4E (*ife-2*) reduces aggregation of Q35-YFP. Images show the head region of day 5-old Q35-YFP nematodes. The control (empty vector) is shown on the left. The scale bars are 10 μm. (**B**) The graph shows a quantification of the number of Q35 aggregates in the whole nematode on day 5 for the control and the knockdown of eIF4G and eIF4E. Error bars represent mean ± standard deviation (s.d.) of 50 animals. (**C**) Western blot of the Q35-YFP protein levels in the control and upon knockdown of eIF4G and eIF4E and control.

the pre-existing levels of Q35-YFP (Figure 7C), from which we conclude that a reduction in bulk protein synthesis is beneficial for cells exposed to protein-folding stress.

Discussion

In this study, we have addressed a role for NAC in maintaining protein homoeostasis in the metazoan *C. elegans*. We show that NAC (i) prevents polyQ aggregation, (ii) is required for maintaining translational activity, (iii) is recruited to protein aggregates formed during diverse conditions of proteotoxic stress including ageing, heat shock, and expression of polyQ proteins and Aβ-peptide, (iv) aids in the resolubilisation of heat-induced aggregates, and (v) is required at the organismal level to survive prolonged exposure to heat. Recuitment of NAC to aggregates always coincided with decreased translational activity similar to the reduced translation caused by RNAi-mediated NAC knockdown. Based on these results, we propose a model that under normal growth conditions, NAC has a primary role as a ribosome-associated chaperone to regulate translation and to assist folding of nascent polypeptides. During ageing and upon exposure to other forms of proteotoxic stress, the appearance of protein aggregates compete for association with NAC, thus reducing the availability of NAC for its ribosomal function to support protein synthesis. This allows NAC to regulate the influx of nascent chains into the cellular proteome, beyond its clients that require NAC's assistance for folding. We therefore suggest that NAC is an essential and beneficial proteostasis sensor that not only detects proteotoxic stress but also mediates the reduction of translation upon proteotoxic stress

conditions to maintain protein homoeostasis (Figure 8). Upon cessation of cell stress and rebalancing of the protein-folding equilibrium, as occurs during recovery from heat shock, NAC re-associates with ribosomes to allow the resumption of protein synthesis (Figure 8, left branch). This model is supported by observations that animals can resume translation and solubilise protein aggregates during recovery from stress. Reduction of NAC function by RNAi however prevents the recovery of translation and heat-shock induced protein aggregates are only partially resolved when NAC is depleted (Figure 4C and D). Chronic stress as represented by the constitutive expression of aggregation-prone proteins or ageing results in the terminal sequestration of NAC, thus depleting NAC from the ribosome causing an irreversible reduction in translation (Figure 8, right branch).

Our observation that the polysome content decreases in animals exposed to proteotoxic stress such as heat shock, expression of disease-associated aggregation-prone polyQ and Aβ and ageing reveals that cells and tissues are constantly monitoring and adjusting their translational capacity in response to proteotoxic perturbations. This is further supported by recent evidence that heat shock and protein misfolding induced by treatment with an amino-acid analogue and proteasome inhibitor cause translational pausing in cell culture that appears to be regulated by Hsp70, thus adding another layer of control for ribosomal activity (Liu *et al*, 2012; Shalgi *et al*, 2012). The mechanism we propose, however, attributes a central role in this new regulatory circuit to the ribosome–associated chaperone complex. We note that the protein levels of α- and βNAC do not change in response to proteotoxic stress or ageing; this supports our
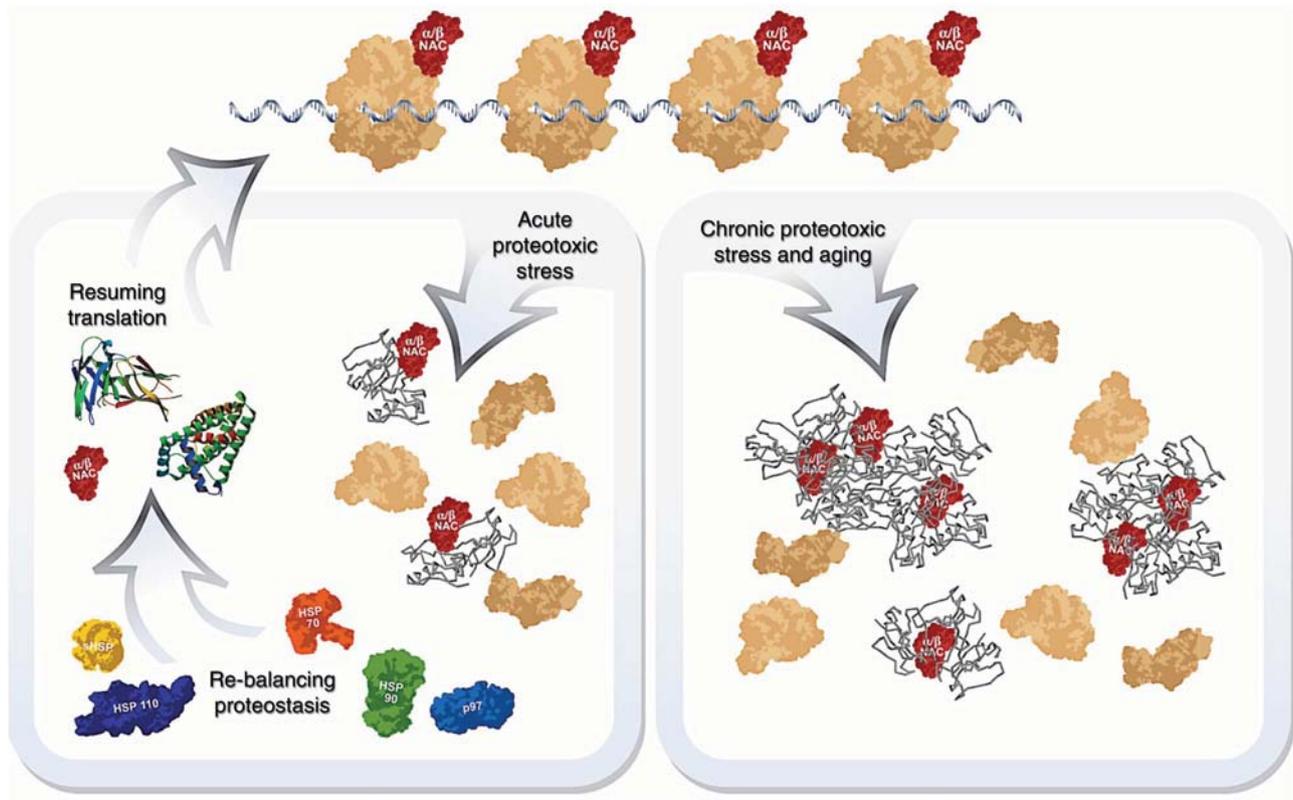
Figure 8 Model for reversible and age/chronic stress-dependent translational control by NAC. Acute proteotoxic challenges (left branch) lead to a temporary translational attenuation due to a sequestration of NAC by misfolded and aggregated proteins. Re-balancing of proteostasis liberates NAC and allows for re-association with ribosomes and translation resumes. Ageing and chronic stress conditions (right branch) lead to a permanent sequestration of NAC and hence to a decrease in protein synthesis.

model that ribosome associated chaperones represent a new class of proteostasis sensors that recognise and respond to proteotoxic challenges. Therefore, the dynamic redistribution of NAC from the soluble to the insoluble protein fraction ensures the fine-tuning of ribosomal activity in response to perturbations of the cellular proteostasis. This point of regulatory control provides a rapid, efficient and reversible response to an imbalance in proteostasis.

Despite the extensive analysis of NAC and its interactions with the ribosome, it remains unknown how NAC mediates the decline of protein synthesis. In the ER, protein-folding stress causes translational attenuation via phosphorylation of eIF2α. Interestingly, a knockdown of NAC leads to an induction of ER Hsp70 ((Arsenovic *et al*, 2012) and data not shown), which is not unexpected as it has been shown that NAC is involved in the co-translational translocation of ER proteins (Wiedmann and Prehn, 1999). In yeast, NAC is required for the early recruitment of SRP to ribosome-nascent chain complexes (RNCs) (Zhang *et al*, 2012). In addition, NAC has been proposed to modulate the binding specificity of SRP, thus indicating a dynamic interplay of NAC and the SRP for the co-translational translocation of RNCs to the ER (del Alamo *et al*, 2011). These observations indicate a connection between the UPR and NAC's function in translational control. However, changes in the phosphorylation of eIF2α have not been observed during ageing of *C. elegans* (Supplementary Figure S9) and have also not been detected upon cytosolic protein misfolding

stress (Liu *et al*, 2012). NAC, therefore, likely provides a new pathway to regulate protein synthesis upon both acute and chronic proteotoxic stress conditions.

How does NAC modulate translation activity? Data from yeast suggest that NAC in cooperation with RAC-Ssb support the biogenesis of the ribosome by maintaining ribosomal proteins in a soluble state (Koplin *et al*, 2010). Indeed, preliminary experiments suggest an involvement of DNJ-11, a putative RAC subunit in *C. elegans* in the regulation of ribosome activity, however additional experiments are required to illuminate the role of RAC in proteostasis (data not shown). Other scenarios are possible as well, for example, NAC might be involved in the control of translation initiation. This hypothesis is supported by an observation that βNAC interacts with the translation initiation factor eIF4E in *Arabidopsis* (Freire, 2005).

Although NAC can become sequestered with aggregated proteins in *ex vivo* experiments, we did not observe a direct interaction of purified NAC with model chaperone substrates such as misfolded and aggregated luciferase and malate dehydrogenase *in vitro* (data not shown). These observations are consistent with the proposal that NAC cooperates with other molecular chaperones in the cell (Figure 8 and Table I). To get additional insight into the endogenous substrate spectrum of NAC, we isolated protein aggregates upon knockdown of βNAC in day 3-old animals and noticed that the functional classes overlap in aggregates from ageing, heat shock and polyQ expression, and are overrepresented

in proteins required for larval development, growth and translation (Fig. Supplementary Figure S10 and Table S4). These data support previous observations of a chaperone function of NAC for ribosomal proteins in yeast (Koplin *et al*, 2010). Notably, we have initial data that the second ribosome-associated chaperone complex, RAC, is also functionally interconnected with NAC and shows similar roles in protein-folding and translation activity. Further attempts will aim at dissecting individual contributions and mechanisms of ribosome-associated chaperones to control protein translation and folding.

Does the attenuation of protein synthesis function as a response to the increased proteotoxic challenges that occur in ageing? We observed that protein synthesis begins to decline from day 3 onwards that corresponds to a period in *C. elegans* devoted to fecundity. During development, the germline maintains a high level of protein synthesis that attenuates during adulthood to adjust to the different requirements of post-mitotic cells and increased risk from stress-induced challenges to cellular proteostasis. This is further supported by observations that the reduction of protein synthesis extends lifespan in *C. elegans* and that certain longevity mutants exhibit reduced protein synthesis (Hansen *et al*, 2007; Pan *et al*, 2007; Syntichaki *et al*, 2007).

The use of *C. elegans* as a model organism provides an experimental system of post-mitotic cells upon completion of development and the reproductive period. Therefore, the proposed model of a chaperone-mediated translational control could extend to other terminally differentiated non-dividing cells and have broad relevance in the biology of ageing. The age-dependent decrease of translation raises important questions whether the decline in translation observed during *C. elegans* development and ageing represents a global event or is tissue selective. Does this lead to translation of selected mRNAs during ageing, even when bulk translation is attenuated? Future studies involving ribosome profiling may help answer this question (Ingolia *et al*, 2009). Likewise, are all tissues affected in parallel and to the same magnitude or are specific cells and tissues more prone to changes in the translational capacity with ageing? The organism-wide translational attenuation observed in *C. elegans* expressing Aβ and polyQ only in muscle cells suggests that a proteostatic decline in one tissue can have widespread consequences.

Materials and methods

Maintenance of *C. elegans*
Nematodes were grown on NGM plates seeded with *E. coli* OP50 strain at 20°C. Animals were synchronized by alkaline hypochlorite treatment. Strains in this study were as follows:

Bristol strain N2 (wild type), AM134 [*rmIs126[Punc-54::q0::yfp]*], AM140 [*rmIs132[Punc-54::q35::yfp]*], AM141 [*rmIs133[Punc-54::q40::yfp]*], CL2006 [*dvIs2[pCL12(unc-54/human Aβ-peptide 1-42 minigene)+pRF4]*], CL2070 [*dvIs70[hsp-16.2::gfp; rol-6(su1006)]*], AM446 [*rmIs[pC12C8.1::GFP; pRF4(rol-6(su1006))]*] and SJ4103 [*zcIs[myo-3::GFP(mit)]*] and AM982 [*rmIs[Punc54::luciferase::yfp]*].

Offspring analysis
Nematodes were singled and transferred onto RNAi plates as L1. To separate them from their progeny, the nematode was passed to a fresh plate every day until no more eggs were laid. The offspring was counted everyday using a Leica mz6 microscope.

Polysome analysis
Synchronized nematode cultures were grown in liquid culture and harvested on ice in 0.1 M NaCl + 100 µg/ml cycloheximide. Nematodes were separated from the *E. coli* food source by sucrose flotation and washed once again in cold 0.1 M NaCl + 100 µg/ml cycloheximide before frozen in liquid nitrogen. Flash frozen *C. elegans* pellets were thawed on ice and resuspended in an equal volume of lysis buffer (30 mM HEPES pH 7.4, 75 mM KoAC, 5 mM MgCl₂, 5% (w/v) mannitol; 100 µg/ml cycloheximide, 2 mM β-mercaptoethanol, 1× Tm Complete protease inhibitor mix (Roche)). Preparation of extract was performed by glass bead disruption (three cycles, 5m/s, 20 s). Alternatively, the frozen animal pellets were ground to powder in a mortar on dry ice and subsequently, resuspend in lysis buffer. After disruption, cell debris was removed by centrifugation at 14 000 *g* at 4°C for 10 min. The resulting lysates were adjusted to an $A_{254\,nm}$ of 20 with lysis buffer. Ten units (500 µl) $A_{254\,nm}$ of each lysate were loaded onto an 11 ml 15–45% (w/v) linear sucrose gradient prepared in lysis buffer (Gradient Master; Biocomp Instruments) and centrifuged for 2.5 h at 39 000 r.p.m. in a swing-out rotor (TH-641; Sorvall) at 4°C. Gradients were fractionated from top to bottom with a density gradient fractionator (Teledyne Isco, Inc.), and A_{254} was monitored to detect cytosolic fraction, ribosomal subunits, monosomes, and polysomes. Data were recorded and processed with PeakTrak V1.1 (Teledyne Isco, Inc.). For one gradient, 24 fractions with 500 µl each were collected. For subsequent western analysis 100 µl of 100% TCA was added to each sample and incubated over night on ice. Proteins were recovered by centrifugation at 14 000 *g* at 4°C for 30 min and the resulting pellets were washed twice in ice-cold acetone. Air-dried pellets were re-suspended in alkaline sample buffer and subsequently separated by SDS–PAGE and then transferred onto a nitrocellulose membrane. Rabbit polyclonal antibodies were raised against purified *C. elegans* NAC, *S. cerevisiae* Rpl17 and *S. cerevisiae* Rpl25. Different dilutions of primary antibodies were applied (1:1000 anti Rpl17 and anti-Rpl25; 1:5000 NAC). Polysome profiles under high-salt conditions were performed as described above with the exception that 1 M KoAc was used in the lysis buffer.

Isolation of protein aggregates
Synchronized *C. elegans* cultures were harvested at day 16 and immediately frozen in liquid N2. The frozen animals were ground to powder in a mortar on dry ice. The efficiency of the lysis was tested by visual inspection of thawed aliquots using a microscope. After successful lysis, the powder was resuspended in ice-cold lysis buffer (20 mM potassium-phosphate, pH 6.8, 10 mM β-mercaptoethanol, 1 mM ethylenediaminetetraacetic acid (EDTA), 0.1% (v/v) Tween 20, protease inhibitor cocktail (Roche)) and centrifuged for 20 min at 200 *g* at 4°C to remove cell debris and residual nematode fragments. The supernatant of multiple samples was adjusted to identical protein concentrations. Aggregated proteins were isolated by spinning at 20 000 *g* for 20 min at 4°C. The resulting pellet was then sonicated (six times at level 4 and duty cycle 50%) in washing buffer (2% NP-40, 20 mM potassium-phosphate, pH 6.8, protease inhibitor cocktail), and subsequently centrifuged at 20 000 *g* for 20 min at 4°C. This step was performed twice. Aggregated proteins were then resuspended in NP-40–deficient washing buffer by sonication (four times at level 2 and duty cycle 65%), pelleted by centrifugation (20 000 *g* for 20 min at 4°C and solubilized in SDS sample buffer at 95°C for 10 min. Proteins were separated by SDS–PAGE (12%) and analysed by Coomassie staining or subsequent immunoblotting.

LC-MS/MS, database searching and data analysis
The SDS PAGE Coommassie blue-stained gel was cut into pieces and subjected to in gel digestion. The extracted peptides were reconstituted in 5% acetonitrile, 0.1% formic acid and analysed by LTQ orbitrap Velos (Thermo Scientific, San Jose, CA). The samples were loaded directly onto 10 cm long, 75 µM reversed phase capillary column (ProteoPep™ II C18, 300 Å, 5 µm size, catalogue number PF7515-100H002, New Objective, Woburn, MA). The peptides were eluted running a 105 min gradient from 5% to 100% acetonitrile on Proxeon Easy n-LC II (Thermo Scientific). The orbitrap velos was operated in data-dependent mode and for each MS1 precursor ion scan (with a resolution of 60 000), the 10 most intense ions were selected from fragmentation by collision induced dissociation. The data were processed using Proteome discoverer (version 1.2,

Thermo Scientific) and searched using in house MASCOT server (http://www.matrixscience.com). The data were searched against UniProtKB/Tremble (Uniprot release 2011_10) with species filter *C. elegans*. All the spectra were searched against target/decoy database and MASCOT significance threshold was chosen to achieve a targeted false discovery rate of 1%. For this analysis, the mascot significance threshold was 0.01. The peptide identification was considered valid if its corresponding mascot score was equal to or less than the threshold.

Titration experiment with aggregates formed during ageing

Aggregates from aged nematodes (day 12) were isolated as described above. However, after the first centrifugation step at $20\,000 \times g$, the pellet of one sample was re-suspended in SDS sample buffer without any additional washing steps ('pre-wash'). A second sample was washed as described above. The supernatants from each washing step were collected and proteins were extracted by TCA precipitation. The resulting pellet was subsequently re-suspended in alkaline sample buffer ('wash'). The pellet after the final washing step ('post-wash') was then re-suspended in protein buffer (30 mM HEPES-KOH pH 7.4, 75 mM potassium acetate, 6 mM magnesium acetate, 2 mM β-mercaptoethanol, Tm complete protease inhibitor cocktail (Roche)) by sonication. The soluble protein fraction was isolated from a synchronized *C. elegans* culture of day 3. For that, the frozen pellet of day 3-old nematodes was ground to powder in a mortar on dry ice and re-suspended in protein buffer. Intact nematodes and aggregates were removed by centrifugation at $20\,000\,g$ for 10 min at 4°C. The supernatant representing the soluble fraction was incubated with 'post-wash' aggregates for 20 min at 20°C. As controls, aggregates and soluble fraction from day 3-old animals alone were incubated and the sample volumes were adjusted with protein buffer; aggregates were re-isolated by centrifugation at $20\,000\,g$ for 20 min at 4°C and immediately solubilized in $2 \times$ SDS–SB for 10 min at 95°C.

Expression and purification of C. elegans NAC

For protein purification of *C. elegans* NAC, pSUMO-NAC was constructed, which expresses the αNAC subunit with an Ulp1-cleavable N-terminal His$_6$-Smt3 tag and the untagged β-subunit, cloned in tandem as one operon. *Y65B4BR.5* (αNAC) and *C56C10.8* (βNAC) genes were cloned into the pSUMO vector. For expression, the plasmid was transformed into the *E. coli* strain BL21(DE3)*/ pRARE. Expression was induced at an $OD_{600\,nm}$ of 0.7 at 30°C with 1 mM isopropyl-1-thio-D-galactopyranoside for 5 h in the presence of appropriate antibiotics. Cells were resuspended in lysis buffer (20 mM sodium phosphate pH 7.5, 300 mM NaCl, 6 mM MgCl$_2$, 2 mM dithiothreitol, 2 mM phenylmethylsulphonyl fluoride, protease inhibitor cocktail (Roche), 10% glycerol) and lysed by French Press. Following centrifugation for 30 min at $30\,000\,g$ at 4°C, the resulting supernatant was applied to Ni-IDA matrix (Protino; Macherey-Nagel) and incubated for 45 min at 4°C. Following high-salt (same as lysis buffer, but with 750 mM NaCl) and low-salt (same as lysis buffer, but with 25 mM NaCl) washes, the bound NAC-complex was eluted in elution buffer (20 mM sodium phosphate pH 7.5, 25 mM NaCl, 6 mM MgCl$_2$, 2 mM DTT, 250 mM imidazole, 10% glycerol) and dialysed overnight in the presence of 4 μg Ulp1 per mg NAC protein for proteolytic cleavage of the His$_6$-Smt3 tag. A final purification step by ion exchange using the Resource Q (Anion exchange) column (GE Healthcare) was used to remove the His$_6$-Smt3 domain, the Ulp and contaminations. Elution fractions containing the α- and β-subunit in a 1:1 ratio (verified by mass spectrometry) were pooled, frozen in liquid nitrogen and stored at -80°C.

Imaging and immunostaining

Nematodes were mounted onto 2% Agarose (Sigma) pads on glass slides and immobilised with 2 mM levamisole (Sigma). Images were taken on Zeiss LSM 510 Meta and on Leica SP5 confocal microscopes. For immunolabeling, nematodes were fixed using paraformaldehyde solution (1 g paraformaldehyde in 25 ml 0.1 M PO$_4$ solution pH 7.2) for 30 min at RT, permeabilized in BME solution (1 ml H$_2$O, 400 μl 0.5 M Tris pH 6.8, 15 μl Triton X-100, 76 μl beta-mercaptoethanol) over night with rotation, washed three times in PBS and treated with collagenase solution (480 μl H$_2$O, 120 μl 1 M Tris pH 7.4, 0.6 μl 1 M CaCl$_2$, 1.2 mg collagenase (Sigma)) for 30 min at 37°C under vigorous agitation. For the staining, the NAC, RPL-4 and RPL-17 antibodies were used in a dilution of 1:100 in

PBS + 0.05% Triton X-100 and 0.1 g/ml BSA and incubated over night at RT. The secondary antibody, Alexa Fluor 546 IgG goat anti-rabbit (Invitrogen) was used in a dilution of 1:100 and incubated for 2 h at RT. DAPI and Mitotracker staining (Hoechst, Molecular Probes; Invitrogen) were carried out in parallel to the incubation with the secondary antibody using a concentration of 10 μg/ml.

RNAi

RNAi of αNAC (*Y65B4BR.5; icd-2*), βNAC (*icd-1*), *ifg-1*, *ife-2*, *hsp-1*, *age-1*, *C12C8.1*, *F11F1.1*, *F44E5.4* and *stc-1* were performed using the feeding vector L4440 to express dsRNA of the respective genes. If not otherwise noted, nematodes were placed as L1 larvae onto RNAi plates and moved to fresh plates every second day to separate them from their progeny. Fifty animals were used for each experimental condition.

Heat shock

Nematodes were subject to heat shock at 35°C for 1 h and either immediately harvested and frozen in liquid nitrogen or transferred to 20°C and continued to grow for 24 h before fixation, harvesting or imaging.

Co-Immunoprecipitation

Fifty microlitres of DYNAL beads (Invitrogen) were cross-linked with 20 μl NAC antibodies according to the manufacturers protocol. For the experiment depicted in Figure 6E, the cross-linked antibodies were then incubated with 50 μg recombinant NAC protein at 4°C for 1 h under rotation. Unbound protein was washed off with PBS. The antibody–antigen complex was then incubated with a total extract of CL2006 at 4°C for 2 h. The antibody–antigen complex was washed three times using 1 ml PBS. Co-precipitated proteins were eluted using PBS pH 3 and subjected to SDS–PAGE and western blot analysis. For the co-immunoprecipitation analysis of NAC depicted in Table I, the cross-linked NAC antibodies were incubated with 2.5 mg of wt lysate and incubated at 4°C for 1 h. After three washing steps using PBS, the co-precipitated proteins were eluted using PBS, pH 3 and subjected to SDS–PAGE. The gel was then stained with Coomassie and visible bands were cut out and analysed by LC-MS/MS.

In vitro titration experiment with heat shock aggregates

For the isolation of ribosomes, polysome profiles were performed as described above with a lysate of day 3-old nematodes. The fractions corresponding to the 80S peak, and the polysomes were pooled from six gradients and dialysed for 2 h at 4°C with ribosome buffer (30 mM HEPES pH 7.4, 75 mM KoAc, 5 mM MgCl$_2$, 5% (w/v) mannitol, 2 mM β-mercaptoethanol). Subsequently, ribosomes were recovered by centrifugation at $200\,000\,g$ for 40 min at 4°C. The resulting ribosomal pellet was re-suspended in 200 μl ribosome buffer ($+2$ mM PMSF), flash frozen in small aliquots in liquid N$_2$ and stored at -80°C until further usage. To generate heat shock aggregates, pellets of day 3-old nematodes were grounded to powder in a mortar on dry ice and re-suspended in aggregate buffer (30 mM HEPES pH 7.4, 100 mM KoAc, 6 mM MgCl$_2$, 1 mM β-mercaptoethanol, $2 \times$ Tm complete protease inhibitor (Roche), 2 mM PMSF). Intact nematodes and debris were removed by centrifugation at $14\,000\,g$ at 4°C for 10 min. The resulting supernatant was adjusted to 1.5 ml with a protein concentration of 5 mg/ml and subsequently centrifuged at $200\,000\,g$ for 40 min at 4°C to pellet ribosomes. The ribosome-free supernatant was then incubated at 42°C for 1 h to form heat shock aggregates. The aggregates were recovered by centrifugation at $40\,000\,g$ for 20 min at 4°C and frozen in liquid N$_2$. To test if NAC can cycle from ribosomes to aggregates, ribosomes were thawed on ice and any precipitations caused by the freezing and thawing steps were removed by centrifugation at $20\,000\,g$ for 40 min at 4°C. The concentration of ribosomes was determined by measuring A260 and 40 pmol of ribosomes were used for the incubation with heat shock aggregates. The heat shock aggregates were thawed and re-suspended in 200 μl ribosome buffer by sonication and 10 μl of the aggregate suspension were directly mixed with the ribosomes for 20 min at 18°C in a volume of 200 μl. As controls, both, the ribosome and aggregate samples were adjusted to 200 μl with ribosome buffer and also incubated at 18°C for 20 min. To recover aggregates the samples were centrifuged at $16\,000\,g$ for 20 min at 4°C (low spin). The pellet was re-suspended in SDS sample buffer and the supernatant was centrifuged at $200\,000\,g$ for 40 min to pellet and isolate ribosomes

(high spin). The ribosomal pellets were then re-suspended in SDS sample buffer. All samples were analysed by SDS–PAGE and subsequent Coomassie staining and western blot.

Western blot analysis

Protein samples were applied to SDS–PAGE and then transferred onto a nitrocellulose membrane according to standard protocols. The blots were analysed using antibodies against NAC (1:5000), Rpl-25 (1:1000), Rpl-17 (1:1000), Rpl-4 (1:750), 4G8 (1:2000; Covance), ubiquitin (1:500; kindly provided by A. Ciechanover), α-tubulin (1:1000, Sigma), Histone H3 (1:1000, Abcam), eIF2α (1:1000; Cell Signalling) and eIF2α-P (1:1000; Cell Signalling). Signals in western blots were quantified using ImageJ software.

Subcellular fractionation

The fractionation into soluble and insoluble proteins shown in Figure 2A was performed as described previously (David *et al*, 2010). Nuclei of *C. elegans* were isolated using differential centrifugation according to a previous study (D'Angelo *et al*, 2009).

Supplementary data

Supplementary data are available at *The EMBO Journal* Online (http://www.embojournal.org).

Acknowledgements

Conflict of interest

The authors declare that they have no conflict of interest.

References

Albanese V, Reissmann S, Frydman J (2010) A ribosome-anchored chaperone network that facilitates eukaryotic ribosome biogenesis. *J Cell Biol* **189:** 69–81

Arsenovic PT, Maldonado AT, Colleluori VD, Bloss TA (2012) Depletion of the *C. elegans* NAC engages the unfolded protein response, resulting in increased chaperone expression and apoptosis. *PLoS One* **7:** e44038

Beatrix B, Sakai H, Wiedmann M (2000) The alpha and beta subunit of the nascent polypeptide-associated complex have distinct functions. *J Biol Chem* **275:** 37838–37845

Ben-Zvi A, Miller EA, Morimoto RI (2009) Collapse of proteostasis represents an early molecular event in *Caenorhabditis elegans* ageing. *Proc Natl Acad Sci U S A* **106:** 14914–14919

Bloss TA, Witze ES, Rothman JH (2003) Suppression of CED-3-independent apoptosis by mitochondrial betaNAC in *Caenorhabditis elegans*. *Nature* **424:** 1066–1071

Buchan JR, Parker R (2009) Eukaryotic stress granules: the ins and outs of translation. *Mol Cell* **36:** 932–941

Bukau B, Deuerling E, Pfund C, Craig EA (2000) Getting newly synthesized proteins into shape. *Cell* **101:** 119–122

Cohen E, Bieschke J, Perciavalle RM, Kelly JW, Dillin A (2006) Opposing activities protect against age-onset proteotoxicity. *Science* **313:** 1604–1610

D'Angelo MA, Raices M, Panowski SH, Hetzer MW (2009) Age-dependent deterioration of nuclear pore complexes causes a loss of nuclear integrity in postmitotic cells. *Cell* **136:** 284–295

David DC, Ollikainen N, Trinidad JC, Cary MP, Burlingame AL, Kenyon C (2010) Widespread protein aggregation as an inherent part of ageing in *C. elegans*. *PLoS Biol* **8:** e1000450

del Alamo M, Hogan DJ, Pechmann S, Albanese V, Brown PO, Frydman J (2011) Defining the specificity of cotranslationally acting chaperones by systematic analysis of mRNAs associated with ribosome-nascent chain complexes. *PLoS Biol* **9:** e1001100

Deng JM, Behringer RR (1995) An insertional mutation in the BTF3 transcription factor gene leads to an early postimplantation lethality in mice. *Transgenic Res* **4:** 264–269

Dorman JB, Albinder B, Shroyer T, Kenyon C (1995) The age-1 and daf-2 genes function in a common pathway to control the lifespan of *Caenorhabditis elegans*. *Genetics* **141:** 1399–1406

Freire MA (2005) Translation initiation factor (iso) 4E interacts with BTF3, the beta subunit of the nascent polypeptide-associated complex. *Gene* **345:** 271–277

Hansen M, Taubert S, Crawford D, Libina N, Lee SJ, Kenyon C (2007) Lifespan extension by conditions that inhibit translation in *Caenorhabditis elegans*. *Ageing Cell* **6:** 95–110

Hartl FU, Hayer-Hartl M (2002) Molecular chaperones in the cytosol: from nascent chain to folded protein. *Science* **295:** 1852–1858

Huang DW, Sherman BT, Lempicki RA (2009a) Bioinformatics enrichment tools: paths toward the comprehensive functional analysis of large gene lists. *Nucleic Acids Res* **37:** 1–13

Huang DW, Sherman BT, Lempicki RA (2009b) Systematic and integrative analysis of large gene lists using DAVID bioinformatics resources. *Nat Protoc* **4:** 44–57

Hundley HA, Walter W, Bairstow S, Craig EA (2005) Human Mpp11 J protein: ribosome-tethered molecular chaperones are ubiquitous. *Science* **308:** 1032–1034

Ingolia NT, Ghaemmaghami S, Newman JR, Weissman JS (2009) Genome-wide analysis *in vivo* of translation with nucleotide resolution using ribosome profiling. *Science* **324:** 218–223

Jaiswal H, Conz C, Otto H, Wolfle T, Fitzke E, Mayer MP, Rospert S (2011) The chaperone network connected to human ribosome-associated complex. *Mol Cell Biol* **31:** 1160–1173

Kemphues KJ, Kusch M, Wolf N (1988) Maternal-effect lethal mutations on linkage group II of *Caenorhabditis elegans*. *Genetics* **120:** 977–986

Koplin A, Preissler S, Ilina Y, Koch M, Scior A, Erhardt M, Deuerling E (2010) A dual function for chaperones SSB-RAC and the NAC nascent polypeptide-associated complex on ribosomes. *J Cell Biol* **189:** 57–68

Lauring B, Sakai H, Kreibich G, Wiedmann M (1995) Nascent polypeptide-associated complex protein prevents mistargeting of nascent chains to the endoplasmic reticulum. *Proc Natl Acad Sci USA* **92:** 5411–5415

Lindquist S (1980) Translational efficiency of heat-induced messages in Drosophila melanogaster cells. *J Mol Biol* **137:** 151–158

Link CD (1995) Expression of human beta-amyloid peptide in transgenic *Caenorhabditis elegans*. *Proc Natl Acad Sci USA* **92:** 9368–9372

Liu B, Han Y, Qian S (2012) Cotranslational response to proteotoxic stress by elongation pausing of ribosomes. *Mol Cell* **49:** 453–463

Markesich DC, Gajewski KM, Nazimiec ME, Beckingham K (2000) Bicaudal encodes the Drosophila beta NAC homolog, a component of the ribosomal translational machinery*. *Development* **127:** 559–572

Moller I, Beatrix B, Kreibich G, Sakai H, Lauring B, Wiedmann M (1998) Unregulated exposure of the ribosomal M-site caused by NAC depletion results in delivery of non-secretory polypeptides to the Sec61 complex. *FEBS letters* **441:** 1–5

Moreau A, Yotov WV, Glorieux FH, St-Arnaud R (1998) Bone-specific expression of the alpha chain of the nascent polypeptide-associated complex, a coactivator potentiating c-Jun-mediated transcription. *Mol Cell Biol* **18:** 1312–1321

Morley JF, Brignull HR, Weyers JJ, Morimoto RI (2002) The threshold for polyglutamine-expansion protein aggregation and cellular

toxicity is dynamic and influenced by ageing in *Caenorhabditis elegans*. *Proc Natl Acad Sci USA* **99:** 10417–10422

Olzscha H, Schermann SM, Woerner AC, Pinkert S, Hecht MH, Tartaglia GG, Vendruscolo M, Hayer-Hartl M, Hartl FU, Vabulas RM (2011) Amyloid-like aggregates sequester numerous meta-stable proteins with essential cellular functions. *Cell* **144:** 67–78

Otto H, Conz C, Maier P, Wolfle T, Suzuki CK, Jeno P, Rucknagel P, Stahl J, Rospert S (2005) The chaperones MPP11 and Hsp70L1 form the mammalian ribosome-associated complex. *Proc Natl Acad Sci USA* **102:** 10064–10069

Pan KZ, Palter JE, Rogers AN, Olsen A, Chen D, Lithgow GJ, Kapahi P (2007) Inhibition of mRNA translation extends lifespan in *Caenorhabditis elegans*. *Ageing Cell* **6:** 111–119

Panniers R (1994) Translational control during heat shock. *Biochimie* **76:** 737–747

Powers T, Walter P (1996) The nascent polypeptide-associated complex modulates interactions between the signal recognition particle and the ribosome. *Curr Biol* **6:** 331–338

Raden D, Gilmore R (1998) Signal recognition particle-dependent targeting of ribosomes to the rough endoplasmic reticulum in the absence and presence of the nascent polypeptide-associated complex. *Mol Biol Cell* **9:** 117–130

Rampelt H, Kirstein-Miles J, Nillegoda NB, Chi K, Scholz SR, Morimoto RI, Bukau B (2012) Metazoan Hsp70 machines use Hsp110 to power protein disaggregation. *EMBO J* **31:** 4221–4235

Raue U, Oellerer S, Rospert S (2007) Association of protein biogenesis factors at the yeast ribosomal tunnel exit is affected by the translational status and nascent polypeptide sequence. *J Biol Chem* **282:** 7809–7816

Reimann B, Bradsher J, Franke J, Hartmann E, Wiedmann M, Prehn S, Wiedmann B (1999) Initial characterization of the nascent polypeptide-associated complex in yeast. *Yeast* **15:** 397–407

Satyal SH, Schmidt E, Kitagawa K, Sondheimer N, Lindquist S, Kramer JM, Morimoto RI (2000) Polyglutamine aggregates alter protein folding homeostasis in *Caenorhabditis elegans*. *Proc Natl Acad Sci USA* **97:** 5750–5755

Shalgi R, Hurt AH, LKrykbaeva I, Taipale M, Lindquist S, Burge CB (2012) Widespread regulation of translation by elongation pausing in heat shock. *Mol Cell* **49:** 439–452

Syntichaki P, Troulinaki K, Tavernarakis N (2007) Protein synthesis is a novel determinant of ageing in *Caenorhabditis elegans*. *Ann NY Acad Sci* **1119:** 289–295

Thiede B, Dimmler C, Siejak F, Rudel T (2001) Predominant identification of RNA-binding proteins in Fas-induced apoptosis by proteome analysis. *J Biol Chem* **276:** 26044–26050

Walter P, Ron D (2011) The unfolded protein response: from stress pathway to homeostatic regulation. *Science* **334:** 1081–1086

Wegrzyn RD, Deuerling E (2005) Molecular guardians for newborn proteins: ribosome-associated chaperones and their role in protein folding. *Cell Mol Life Sci* **62:** 2727–2738

Wiedmann B, Prehn S (1999) The nascent polypeptide-associated complex (NAC) of yeast functions in the targeting process of ribosomes to the ER membrane. *FEBS Lett* **458:** 51–54

Wiedmann B, Sakai H, Davis TA, Wiedmann M (1994) A protein complex required for signal-sequence-specific sorting and translocation. *Nature* **370:** 434–440

Yotov WV, Moreau A, St-Arnaud R (1998) The alpha chain of the nascent polypeptide-associated complex functions as a transcriptional coactivator. *Mol Cell Biol* **18:** 1303–1311

Zhang Y, Berndt U, Golz H, Tais A, Oellerer S, Wolfle T, Fitzke E, Rospert S (2012) NAC functions as a modulator of SRP during the early steps of protein targeting to the endoplasmic reticulum. *Mol Biol Cell* **23:** 3027–3040